UNIVERSITY OF CALGARY

Characterization of the Fifth Member of the Potassium-dependent Sodium/Calcium Exchanger Family – NCKX5

by

Guang Yang

A THESIS

SUBMITTED TO THE FACULTY OF GRADUATE STUDIES

IN PARTIAL FULFILMENT OF THE REQUIREMENTS FOR THE

DEGREE OF MASTER OF SCIENCE

DEPARTMENT OF BIOCHEMISTRY AND MOLECULAR BIOLOGY

CALGARY, ALBERTA

APRIL, 2007

UNIVERSITY OF CALGARY

FACULTY OF GRADUATE STUDIES

The undersigned certify that they have read, and recommend to the Faculty of Graduate Studies for acceptance, a thesis entitled "Characterization of the Fifth Member of the Potassium-dependent Sodium/Calcium Exchanger Family – NCKX5" submitted by Guang Yang in partial fulfilment of the requirements of the degree of Master of Science.

Supervisor, Dr. Jonathan Lytton
Department of Biochemistry and Molecular Biology

Dr. Andrew P. Braun
Department of Cardiovascular/Respiratory Sciences

Dr. S.R. Wayne Chen
Department of Cardiovascular/Respiratory Sciences

Dr. Gary J. Kargacin
Department of Cardiovascular/Respiratory Sciences

Date

ABSTRACT

Cellular Ca^{2+} homeostasis is vital for cell survival and various cellular processes. Potassium-dependent sodium/calcium exchangers (NCKX) play an important role in maintaining cellular Ca^{2+} homeostasis. The fifth isoform of K^+-dependent Na^+/Ca^{2+} exchanger (NCKX5), a newly discovered member, is thought to be involved in melanosome biogenesis and pigmentation.

The overall aim of this project is to characterize mouse NCKX5 at the molecular level. Northern blotting revealed two major transcripts with variable expression in several mouse tissues and B16 melanoma cells. Using an anti-NCKX5 antibody, I demonstrated by immunoblot the expression of the NCKX5 protein in transfected HEK293 cells, B16 and MNT1 cells. Two major bands were observed as a result of different glycosylation states. Immunofluorescence analysis showed that the NCKX5 protein was localized at the perinuclear region. Microsomes from B16 and MNT1 cells displayed NCKX activity measured using Ca^{2+} uptake.

ACKNOWLEDGEMENTS

My deepest gratitude goes first to my supervisor, Dr. Jonathan Lytton, for his invaluable guidance, constant encouragement and patience during my study. I would like to thank the members of my supervisory committee, Dr. Andrew P. Braun and Dr. S.R. Wayne Chen, for their precious suggestions on my research project. I would also like to give my thanks to Yiqian Wang, Xiaofang Li, and Frank Visser for their valuable help in my project and all the other members in our laboratory, Sally Yoo, Liao Liao and Charu Chandrasekera for their kindness and friendness. Finally, I would like to express my appreciation to my parents and all my friends for their continuous support and care for me.

Dedicated to my parents

TABLE OF CONTENTS

LIST OF TABLES

LIST OF FIGURES

LIST OF SYMBOLS AND ABBREVIATIONS

Symbol	Definition
AP	Adaptor protein
ATP	Adenosine triphosphate
DCT	Dopachrome tautomerase
DHI	5,6-dihydroxyindole-melanin
DNA	Deoxyribonucleic acid
cDNA	Complementary DNA
DOPA	3,4-dihydroxyphenylalanine
DMEM	Dulbecco's modified Eagle's medium
DTT	Dithiothreitol
EDTA	Ethylene glycol-*bis*(β-amino-ethyl)-N,N,N',N',-tetra-acetic acid
ER	Endoplasmic reticulum
FBS	Fetal bovine serum
HEK293	Human embryonic kidney cell line
$InsP_3$	Inositol 1,4,5-triphosphate
$InsP_3R$	Inositol 1,4,5-triphosphate receptor
NCKX	Potassium-dependent sodium/calcium exchanger
NCX	Potassium-independent Sodium/calcium exchanger
NEAA	Non-essential amino acid
PBS	Phosphate buffered saline
PCR	Polymerase chain reaction

PIP_2	Phosphatidylinositol 4,5-bisphosphate
PKA	Protein kinase A
PKC	Protein kinase C
PLC	Phospholipase C
PLN	phospholamban
PMCA	Plasma membrane Ca^{2+}-ATPase
PMSF	Phenylmethanesulfonyl fluoride
RNA	Ribonucleic acid
RPE	Retinal pigment epithelium
RT-PCR	Reverse transcription coupled polymerase chain reaction
RyR	Ryanodine receptor
SDS	Sodium dodecyl sulphate
SDS-PAGE	Sodium dodecyl sulphate-polyacrylamide gel electrophoresis
SERCA	Sarcoplasmic reticulum/ endoplasmic reticulum Ca^{2+}-ATPase
SOC	Store-operated Ca^{2+} channel
SPCA	Secretory-pathway Ca^{2+}-ATPase
SR	Sarcoplasmic reticulum
STIM	Stromal interacting molecule
TGN	*Trans*-Golgi network
TYRP	Tyrosinase-related protein
XIP	Exchanger inhibitory peptide

CHAPTER ONE

INTRODUCTION

1.1 The importance of calcium ion

Calcium is one of the most important elements in living creatures (Berridge, Bootman et al. 1998). It is well known that calcium makes bones and teeth strong. Furthermore, ionized calcium (Ca^{2+}) is also one of the vital intracellular signaling molecules in virtually all types of cells (Bootman, Collins et al. 2001). Ca^{2+} entering into the intracellular environment can trigger or regulate various cellular processes (Bootman, Collins et al. 2001). Changes in intracellular Ca^{2+} concentration ($[Ca^{2+}]_i$) control cell fertilization, differentiation, and development. Ca^{2+} also mediates cell growth, gene transcription, hormone secretion, vesicle trafficking, neurotransmitter release, as well as muscle contraction and relaxation (Berridge, Lipp et al. 2000). Thus, Ca^{2+} controls almost everything our bodies do, such as movement, heart beat, information processing in the brain, learning and memory (Berridge, Bootman et al. 1998).

Ca^{2+} can play such an important role partly because it is one of the most prevalent divalent cations in cells (Berridge, Bootman et al. 1998). Moreover, in resting cells, intracellular calcium concentration is maintained at a very low level, about 10 to 100nM (Berridge, Lipp et al. 2000). When resting cells are stimulated, Ca^{2+} enters these cells through plasma membrane calcium channels or is released from intracellular Ca^{2+} stores such as the endoplasmic reticulum (ER) and sarcoplasmic reticulum (SR), so that the intracellular Ca^{2+} concentration can rise up to tens of μM transiently (Bootman, Collins et

al. 2001; Petersen 2002). Therefore, a large signal-to-background ratio is achieved (Bootman, Collins et al. 2001).

However, $[Ca^{2+}]_i$ must be precisely controlled to meet different needs of various cell types (Berridge, Bootman et al. 1998). In many cases, like cardiac muscle contraction and the transient release of neurotransmitter substances, the increased $[Ca^{2+}]_i$ is required for only short periods of time. This free intracellular Ca^{2+} must be then removed very rapidly from the cells. In other instances, such as the maintenance of tonic tension of smooth muscle, the elevated $[Ca^{2+}]_i$ may be required for a longer time. Therefore, modulation of $[Ca^{2+}]_i$ must allow both a fast increase and decrease to provide a transient signal, and a gradual change to provide a relatively steady signal (Bootman, Collins et al. 2001). Besides the temporal differences of $[Ca^{2+}]_i$, in some other cells there must also be spatial variation in $[Ca^{2+}]_i$ so that multiple calcium-regulated processes are not activated simultaneously (Berridge, Bootman et al. 1998). The precise control of intracellular Ca^{2+} concentration is therefore essential for providing specificity of signaling (Bootman and Berridge 1995; Berridge, Bootman et al. 2003).

1.2 Ca^{2+} entry and release mechanisms

Intracellular Ca^{2+} concentration rises through two ways: (1) extracellular free Ca^{2+} flows into cells upon stimuli through Ca^{2+} entry channels located on the plasma membrane (Bootman, Collins et al. 2001), or (2) Ca^{2+} is released from intracellular Ca^{2+} stores (Bootman and Berridge 1995).

1.2.1 Ca^{2+} entry channels

Cell surface Ca^{2+} entry channels can be grouped into several types according to their activation mechanisms (Berridge, Lipp et al. 2000).

The first type are voltage-gated Ca^{2+} channels (Berridge, Lipp et al. 2000), which have been studied most intensively so far. This type of channel is activated by depolarization of the plasma membrane (Berridge, Lipp et al. 2000) and is largely found in excitable cells, such as myocytes and neurons (Bootman, Collins et al. 2001). Voltage-gated Ca^{2+} channels usually consist of a major pore-forming subunit in association with other auxiliary subunits which regulate channel gating (Bootman and Berridge 1995).

The second type are store-operated Ca^{2+} channels (SOC) (Berridge, Lipp et al. 2000), which are more ubiquitously expressed in many different types of cells. This type of channel is activated upon depletion of intracellular Ca^{2+} stores, either by physiological Ca^{2+} messengers or by pharmacological agents (Berridge, Lipp et al. 2000; Bootman, Collins et al. 2001). Two proteins, stromal interacting molecule isoform 1 (STIM1) (Roos, DiGregorio et al. 2005) and Orai1 (Feske, Gwack et al. 2006), are proposed to play a key role in controlling Ca^{2+} influx through store-operated Ca^{2+} channels. It has been suggested that Orai1 may form the store-operated Ca^{2+} channel itself (Soboloff, Spassova et al. 2006) and STIM1 may function as the sensor of luminal Ca^{2+} concentration changes (Liou, Kim et al. 2005).

The third type are receptor-operated channels, which are mainly found on secretory cells and at nerve terminals (Bootman, Collins et al. 2001). They comprise a wide range of structurally and functionally diverse channels, which open or close in response to the

binding of ligands or their agonists, such as ATP, glutamate, or acetylcholine (Berridge, Lipp et al. 2000).

The fourth type are mechanically activated Ca^{2+} channels which are also present in many cell types. This type of channel conveys information regarding the stress or shape changes that cells are experiencing and responds to cell deformation (Bootman, Collins et al. 2001).

The fifth type are second messenger-gated Ca^{2+} channels, exemplified by the cGMP gated Ca^{2+} channel, found in rod and cone photoreceptor cells. This channel opens when cGMP binds to it and closes when the cGMP concentration decreases (Decressac, Grechez-Cassiau et al. 2002).

1.2.2 Ca^{2+} release channels

The largest intracellular Ca^{2+} stores are found in the ER/SR and there are several kinds of Ca^{2+} release channels located on the ER/SR membrane (Berridge, Lipp et al. 2000). One type is inositol 1,4,5-triphosphate receptor ($InsP_3R$), which is ubiquitously expressed in mammalian cells (Bootman, Collins et al. 2001). $InsP_3Rs$ are large structures composed of four subunits, and three different genes encoding these subunits have been discovered. $InsP_3Rs$ are gated by $InsP_3$ binding and by the Ca^{2+} concentration at their cytosolic side. $InsP_3Rs$ opening is enhanced by modest increases in Ca^{2+} concentration (0.5-1μM) whereas higher Ca^{2+} concentration (over 1μM) inhibits their opening (Bootman, Collins et al. 2001). This dependence of $InsP_3Rs$ activity on cytosolic Ca^{2+} is crucial for the generation of the complex patterns of Ca^{2+} signals seen in many cells (Berridge, Lipp et al. 2000).

The other type of Ca^{2+} release channel are ryanodine receptors (RyRs), which are so-named because of their high affinity for the plant alkaloid ryanodine (Berridge, Bootman et al. 2003). RyRs are sensitive to Ca^{2+} concentration at the cytosolic side. They are activated at 1-10μM and inhibited when $[Ca^{2+}]_i$ is over 1mM (Bootman, Collins et al. 2001). Luminal Ca^{2+} concentration can regulate the gating of RyRs too. Rising luminal Ca^{2+} concentration can increase the open probability of RyRs. (Gyorke, Hester et al. 2004). RyRs are structurally and functionally analogous to $InsP_3Rs$, but have approximately twice the conductance and molecular mass of $InsP_3Rs$ (Berridge, Lipp et al. 2000). Unlike $InsP_3Rs$, RyRs are largely present in excitable cells, such as muscle cells and neurons. There are three isoforms of RyR proteins that are expressed in different types of cells. Different isoforms of RyRs have different mechanisms for triggering Ca^{2+} release (Laver 2006; Kong, Wang et al. 2007).

1.3 Ca^{2+} removal and sequestration mechanisms

Prolonged high $[Ca^{2+}]_i$ can be toxic, even leading to cell death (Berridge, Bootman et al. 1998). Thus, after triggering and regulating these signaling events, proper Ca^{2+} extrusion or sequestration is vital to all cells (Berridge, Lipp et al. 2000). Ca^{2+} leaves the cytosolic environment in two different directions: either by being sequestered back into intracellular stores, or by being extruded out of the cells. These processes are carried out by different proteins located on the membrane of the internal Ca^{2+} stores, such as the SR/ER Ca^{2+}-ATPase (SERCA), or on the plasma membranes, i.e. the plasma membrane Ca^{2+}-ATPase (PMCA) and the sodium/calcium exchangers (NCX/NCKX) (Berridge, Lipp et al. 2000; Berridge, Bootman et al. 2003).

Internal Ca^{2+} stores are associated with the SR/ER, mitochondria, and Golgi apparatus. It is thought that the secretory-pathway Ca^{2+}-ATPase (SPCA) is responsible for Ca^{2+} uptake into the Golgi apparatus (Berridge, Bootman et al. 2003). Mitochondria have a substantial capacity for Ca^{2+} uptake and can significantly buffer cytosolic Ca^{2+}. Mitochondria sequester Ca^{2+} through a low-affinity, high-speed uniporter driven by the negative mitochondria membrane potential (Berridge, Lipp et al. 2000). Besides Golgi apparatus and mitochondria, the ER and SR play a vital role in Ca^{2+} sequestration. SERCA carries out the task of pumping cytosolic Ca^{2+} into SR/ER. In resting cardiac cells, smooth or slow-twitch skeletal muscles, a small molecule phospholamban (PLN) is associated with SERCA and inhibits SERCA activity. Phosphorylation of PLN by PKA, which is activated through the β-adrenergic pathway, causes the dissociation of PLN from SERCA. The dissociation of PLN increases the activity and affinity of SERCA for Ca^{2+} and initiates the process of SERCA pumping Ca^{2+} back into SR/ER (Berridge, Lipp et al. 2000; Rossi and Dirksen 2006). Inside SR/ER, free Ca^{2+} is buffered by small Ca^{2+} binding proteins, such as calnexin, calreticulin, and calsequestrin (Berridge, Bootman et al. 2003).

PMCA plays an important role in pumping Ca^{2+} out of cells. It is powered by the hydrolysis of adenosine triphosphate (ATP), with a stoichiometry of one Ca^{2+} ion removed for each molecule of ATP hydrolyzed (Berridge, Lipp et al. 2000). It has a high affinity for Ca^{2+}, but a low Ca^{2+} removal rate. Thus PMCA is effective at binding Ca^{2+} even when its concentration within the cell is very low, so PMCA is suited for maintaining Ca^{2+} at its normally low resting levels. Ca^{2+} or calmodulin binds and further

activates PMCA, increasing the affinity of the protein's Ca^{2+} binding site 20 to 30 times (Berridge, Bootman et al. 2003; Strehler and Treiman 2004).

1.4 Sodium/Calcium exchanger gene family

The Na^{+}/Ca^{2+} exchange activity was first identified in squid axons and cardiac myocytes in 1968 and 1969 (Reuter and Seitz 1968; Baker, Blaustein et al. 1969). Later, Na^{+}/Ca^{2+} exchangers were found in many other cell types including neurons, glia, and smooth muscle cells, where they play a key role in controlling plasma membrane Ca^{2+} efflux (Philipson and Nicoll 2000). In contrast to PMCA, Na^{+}/Ca^{2+} exchangers have a low affinity for Ca^{2+} but a high Ca^{2+} transport rate. Therefore, they are better suited for removing large amounts of Ca^{2+} quickly, as is needed in neurons after an action potential (Berridge 1998; Blaustein and Lederer 1999). The activities of PMCA and Na^{+}/Ca^{2+} exchangers seem to complement each other. Both of them are key players in maintaining intracellular Ca^{2+} homeostasis.

Based upon the amino acid similarity and ion transport specificities of the molecules, the Na^{+}/Ca^{2+} exchanger family can be further divided into two different subfamilies: one is K^{+}-independent Na^{+}/Ca^{2+} exchangers, *SLC8* (NCX), and the other is K^{+}-dependent Na^{+}/Ca^{2+} exchangers, *SLC24* (NCKX), in which K^{+} is a requirement for Ca^{2+} transport (Blaustein and Lederer 1999). The members in these two subfamilies share an amino acid similarity only in two short stretches, named the α-repeats, one in each hydrophobic helix cluster, that have apparently been conserved during evolution (Lennarz and Lane 2004).

The proposed overall topological structure of all the known members in the sodium/calcium exchanger family is quite similar: beginning with a solitary

transmembrane segment, which is removed as a "signal peptide", a short extracellular loop, followed by the first hydrophobic cluster of five transmembrane-spanning segments (TMS), a long cytoplasmic loop, and ending with the second hydrophobic cluster of four or five transmembrane-spanning segments (four TMS for NCX members and five TMS for NCKX members) (Blaustein and Lederer 1999; Philipson and Nicoll 2000; Cai, Zhang et al. 2002; Cai, Zhang et al. 2002; Kinjo, Szerencsei et al. 2003) (Figure 1).

As their names imply, the members in NCX subfamily utilize the Na^+ concentration gradient across the membrane to actively transport Ca^{2+} (Philipson and Nicoll 2000), whereas the members in NCKX subfamily use both the Na^+ and the K^+ concentration gradients to transport Ca^{2+} (Schnetkamp 2004). The transport is bidirectional and the direction of the ion movement depends upon the net electrochemical gradients of the ions and the coupling ratio (Lennarz and Lane 2004). Under most physiological conditions, the members in NCX subfamily extrude Ca^{2+} out of cells while taking sodium ions into cells and the members in NCKX subfamily extrude Ca^{2+} and K^+ out of cells while taking Na^+ into cells (forward mode). If the ion concentration gradients are changed, Ca^{2+} may also be transported into the cells (reverse mode). An example is in the erythrocytes of dogs, where the Na^+/Ca^{2+} exchanger plays an important role in the extrusion of Na^+ (Blaustein and Lederer 1999; Philipson and Nicoll 2000; Szerencsei, Winkfein et al. 2002).

1.4.1 Potassium-independent sodium/calcium exchangers (NCX)

The NCX subfamily is thought to transport three or four Na^+ ions in exchange for one Ca^{2+} ion (Blaustein and Lederer 1999; Lytton 2002). There are three known genes in

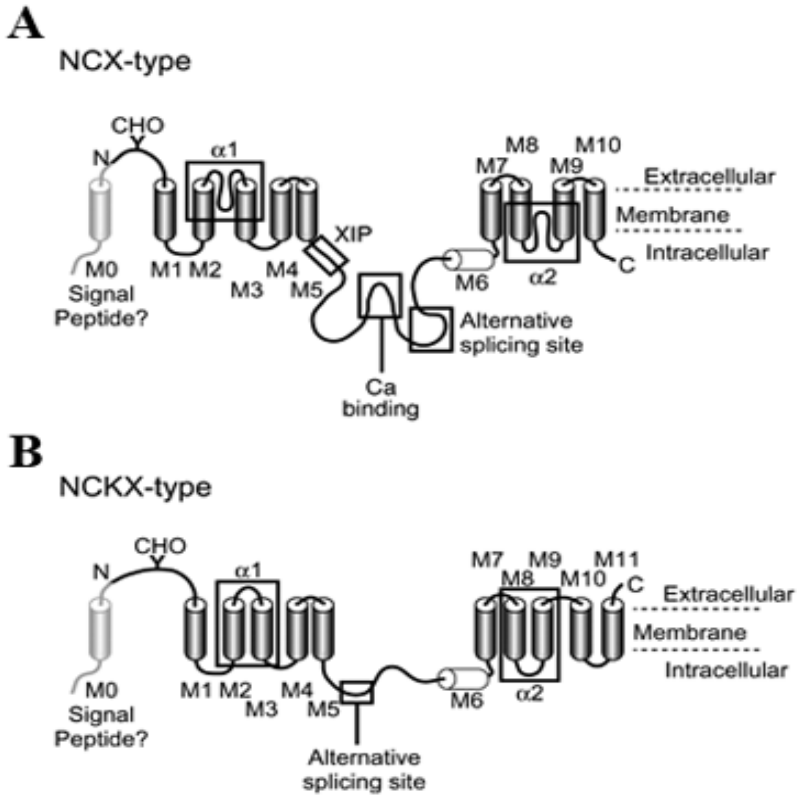

Figure 1. Proposed topological structures of NCX and NCKX. A shows the proposed topological structure of NCX. **B** shows the proposed topological structure of NCKX. The two sides of the membrane are labeled so that they can be distinguished. Transmembrane segments are labeled as M0 to M10 (NCX) or M11 (NCKX). Note that M6, although hydrophobic in nature, is not thought to span the membrane. The first transmembrane segment is shaded as it is predicted to be cleaved as a signal peptide. N: the signal peptidase cleavage site; CHO: the N-glycosylation site; α1 and α2: two α-repeats. Regulatory Ca^{2+} binding site and the exchanger inhibitory peptide (XIP) region for NCX and alternative splicing sites are all boxed and labeled. Figure adapted from Lytton, J. Membrane Transporters: Na+/Ca2+ exchangers. In Lennarz, W.J. & Lane M.D., eds. *Encyclopedia of Biological Chemistry* Elsevier, Oxford, 2004; Vol. 2; pp. 631-636

this subfamily, NCX1, NCX2, and NCX3, whose protein products share a high degree of identity, especially in the transmembrane regions (Philipson and Nicoll 2000). NCX1, the first member of the whole Na^+/Ca^{2+} exchanger family to be found, was first isolated and cloned from canine cardiac sarcolemma. The coding region of mouse NCX1 cDNA contains 2,910 base pairs (bp) and encodes a 970-amino-acid protein. However, the mature NCX1 protein is 938 amino acids long, as the first 32 amino acids are cleaved by a signal peptidase during the initial processing in the ER, where the NCX1 protein is glycosylated as well (Nicoll, Longoni et al. 1990). NCX2 and NCX3 were cloned subsequently based on homology to NCX1. The mouse NCX2 cDNA open reading frame consists of a sequence of 2,763bp, encoding a protein of 921 amino acids (Li, Matsuoka et al. 1994). Mouse NCX3 protein, which is encoded by a sequence of 2,784 nucleotides cDNA segment, is 928 amino acids long (Nicoll, Quednau et al. 1996). NCX1 and NCX3 genes, but not NCX2, are alternatively spliced to produce tissue-specific protein isoforms in which a small region in the cytoplasmic loop of the exchanger is altered (Quednau, Nicoll et al. 1997).

In the large cytoplasmic loop of NCX1, several regulatory sites exist, such as the Ca^{2+} regulatory site and the exchanger inhibitory peptide (XIP) region (Figure 1A), which is 20 amino acids in length (Philipson and Nicoll 2000) at the extreme N-terminus region of the loop (Lennarz and Lane 2004). A peptide with the same sequence as the XIP region has an inhibitory effect on the exchange activity (Philipson and Nicoll 2000). Different factors regulate the exchange activity through these sites. Ca^{2+} binding to the Ca^{2+} regulatory site is not transported but functions to activate the exchanger (Philipson and Nicoll 2000) while a high concentration of Na^+ at the intracellular side causes

inactivation (Blaustein and Lederer 1999), termed Na^+-dependent inactivation. Mutations in the XIP region dramatically affect the Na^+-dependent inactivation (Philipson and Nicoll 2000). PIP_2 and ATP can also activate exchange activity through the XIP region (Lennarz and Lane 2004).

The tissue distribution patterns of the three NCX family members are distinct. NCX1, with a 7kb transcript, is known to be highly expressed in cardiac muscle and to a less degree in many other tissues, such as kidney, brain, skeletal muscle, smooth muscle, and spleen (Nicoll, Longoni et al. 1990). The sizes of the transcripts of NCX2 and NCX3 are 5kb (Li, Matsuoka et al. 1994) and 6kb (Nicoll, Quednau et al. 1996) respectively. NCX2 is most abundantly expressed in brain with a lower expression in skeletal muscle (Li, Matsuoka et al. 1994) while NCX3 is highly expressed in skeletal muscle with a lower expression in selected brain regions (Nicoll, Quednau et al. 1996). However, their molecular properties have not been investigated as thoroughly as those of NCX1 (Philipson and Nicoll 2000).

1.4.2 Potassium-dependent Sodium/Calcium Exchangers (NCKX)

The NCKX subfamily is thought to transport four Na^+ ions in exchange for one Ca^{2+} ion and one K^+ ion (Dong, Light et al. 2001; Lytton, Li et al. 2002). Five members of this subfamily have been identified, named from NCKX1 to NCKX5 (Schnetkamp 2004). All of them display high identity and similarity at the amino acid level in the two hydrophobic transmembrane segment clusters surrounding the two "α-repeats", whereas in the large cytoplasmic loop, they show little amino acid similarity (Lennarz and Lane 2004) (Figure 2).

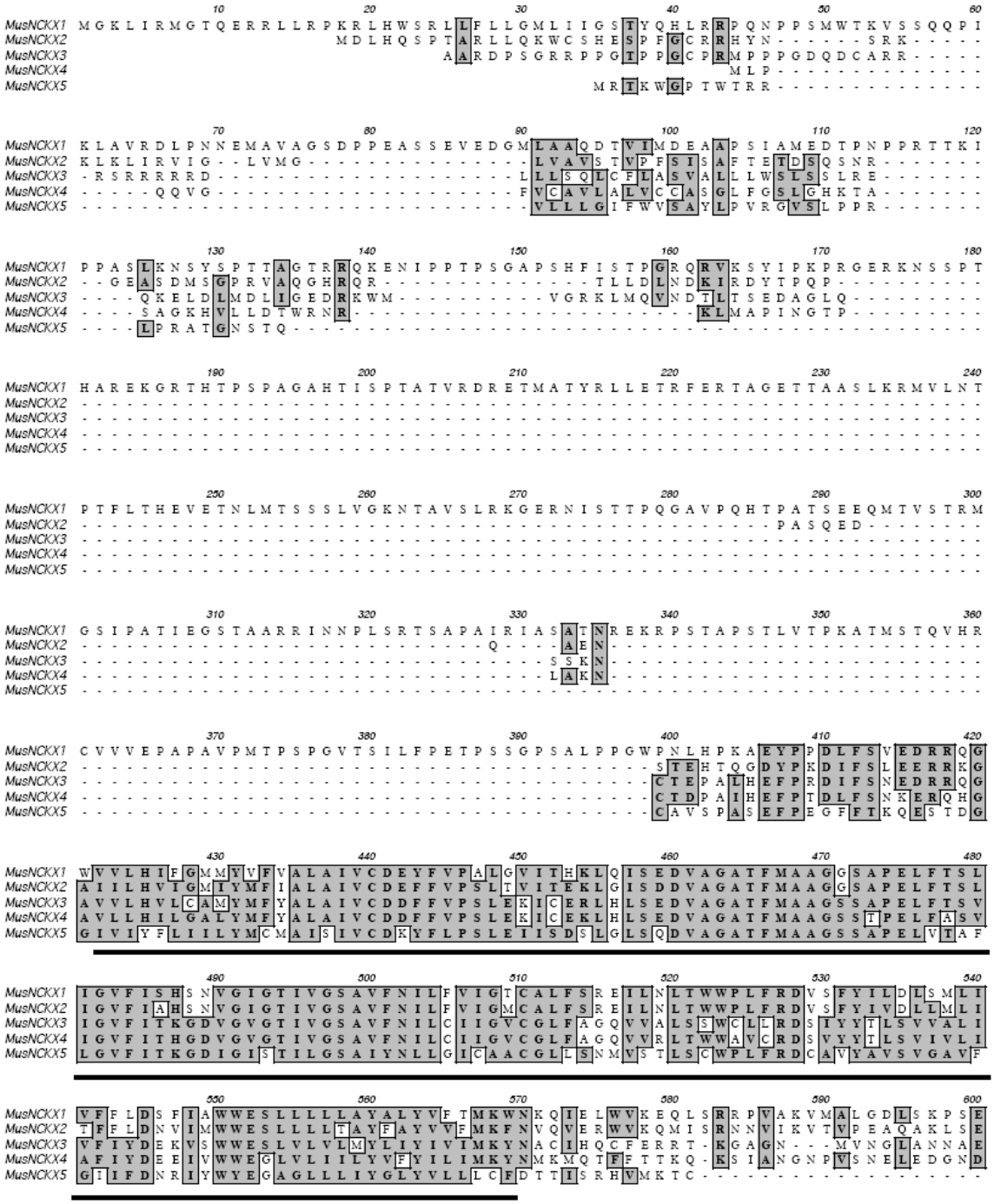

Figure 2. Alignment of mouse NCKX amino acid sequences. Conserved amino acid residues are boxed and shaded. Two clusters of transmembrane-spanning segments are underlined.

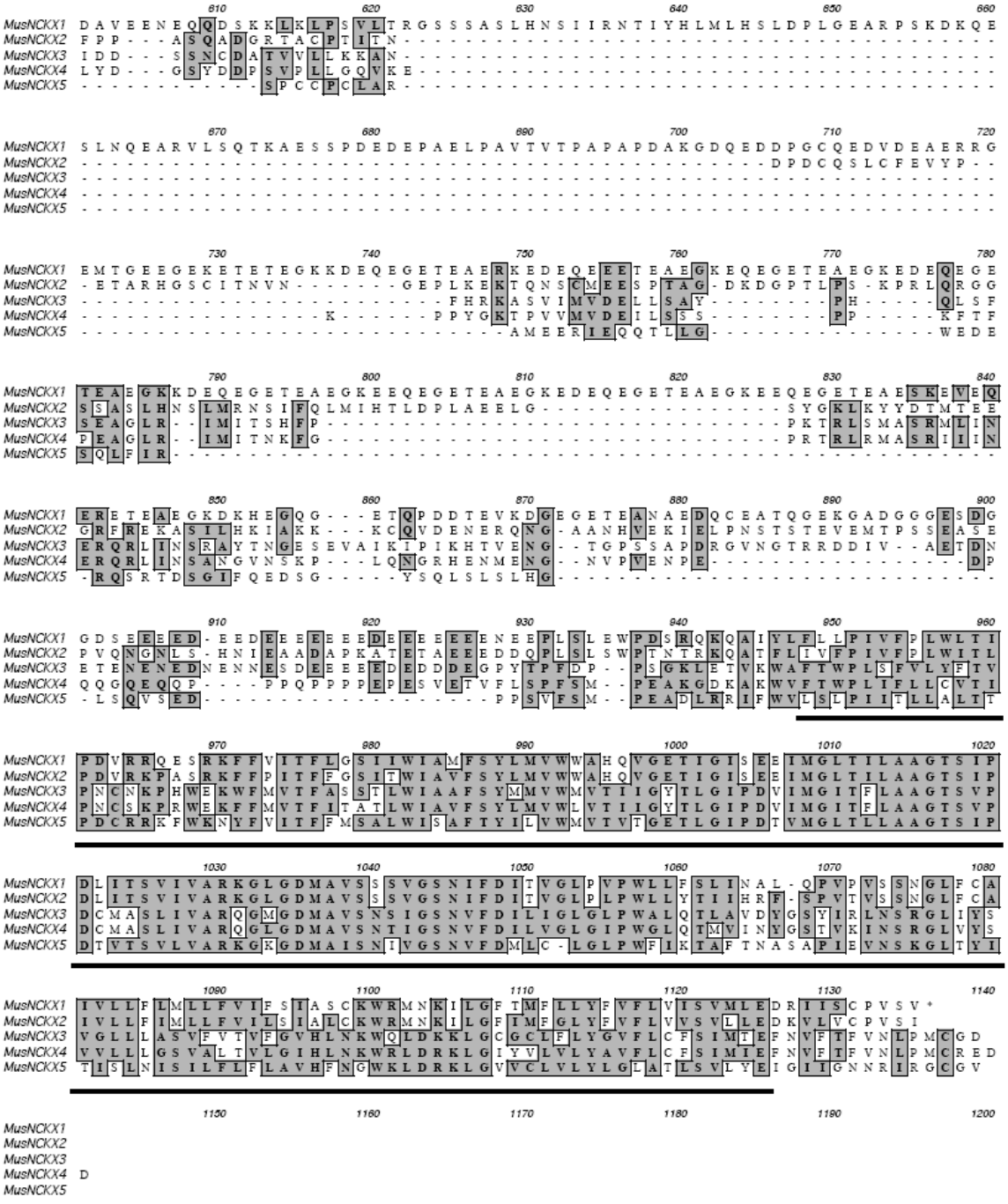
MusNCKX1
MusNCKX2
MusNCKX3
MusNCKX4
MusNCKX5

NCKX1 was first discovered in the outer segments of vertebrate rod photoreceptors (Cervetto, Lagnado et al. 1989) where it is the only mechanism for extruding Ca^{2+} that enters rod photoreceptors through the light-sensitive cGMP-gated channels (Schnetkamp 2004). It also was the first member of this family to be cloned, from bovine retina (Cook and Kaupp 1988). NCKX2 was then found and cloned from rat brain (Tsoi, Rhee et al. 1998). NCKX3 and NCKX4 were found by homology with NCKX1 using bioinformatic methods and were cloned as well (Kraev, Quednau et al. 2001; Li, Kraev et al. 2002). Some mammalian NCKX homologues from invertebrate species, such as *drosophila* and *C. elegans*, have also been identified and cloned. All the four members have two or more alternatively spliced isoforms (Lennarz and Lane 2004; Schnetkamp 2004). So far, NCKX1 and NCKX2 are the only two members in this subfamily which have been studied intensively.

The open reading frame of NCKX1 contains about 3.6kb. The NCKX1 protein has a deduced sequence containing about 1,200 amino acids and a calculated molecular weight of around 130kDa. The NCKX1 mRNA expression is restricted to a 6kb transcript existing only in the eye (Reilander, Achilles et al. 1992; Blaustein and Lederer 1999; Philipson and Nicoll 2000; Schnetkamp 2004).

The coding region of NCKX2 cDNA is around 2kb long and encodes a protein of 666 amino acids which has a molecular weight around 75kDa (Tsoi, Rhee et al. 1998). It has been reported that NCKX2 may form oligomers (Yoo, Leach et al. 2002). NCKX2 has two major transcripts. The 10.5kb one is highly expressed in all regions of brain with a lower level of expression in cone photoreceptors and retinal ganglion cells, and also at a

very low level in large intestine, and adrenal gland. Another NCKX2 transcript of about 4.5kb is expressed in heart, aorta, small and large intestine, as well as lung but all at much lower levels compared to the 10.5kb transcript in brain (Tsoi, Rhee et al. 1998).

The Mouse NCKX3 transcript is 4.5kb in length with the coding region of 1.8kb giving a mature protein product of 595 amino acids and a size of about 65kDa. NCKX3 transcripts are most abundantly expressed in various brain regions, aorta, intestine, and lung. Lower levels of expression were found in many other tissues whereas almost no expression was detected in liver and kidney (Kraev, Quednau et al. 2001).

The open reading frame of mouse NCKX4 contains 1,815 nucleotides encoding a 605-amino-acid protein product with the calculated size of 67kDa (Li, Kraev et al. 2002). NCKX4 has three transcripts, 10kb, 4.5kb, and 2.5kb respectively. The major transcript is the 10kb one which is expressed abundantly in various brain regions, aorta, lung, and thymus with lower expression levels in various tissues such as heart, kidney, smooth muscle, and skeletal muscle. The 4.5kb and 2.5kb transcripts are more widely expressed although liver has essentially no NCKX4 expression (Li, Kraev et al. 2002) (Table 1). These unique and non-overlapping expression patterns of different NCKX members suggest they each play a specialized role in Ca^{2+} signaling in different cell types and tissues (Lennarz and Lane 2004).

Functional and kinetic studies have been conducted on NCKX1 and NCKX2. The results demonstrated that the basic transport characteristics of these two molecules are very similar (Schnetkamp 2004). Na^+ is required for the transport and cannot be replaced by any other cations, whereas K^+ can be replaced by Rb^+ or NH_4^+ but not by Cs^+ or Li^+.

Table 1 Tissue distribution pattern and transcript size of NCKX members

Gene	Transcript size	Tissue distribution
NCKX1	6kb	Strictly in eye
NCKX2	10.5kb	Mainly in all regions of brain
	4.5kb	Heart, aorta, small and large intestine, and lung
NCKX3	4.5kb	Widely expressed Mainly in various brain regions, aorta, intestine, and lung but no expression in liver and kidney
NCKX4	10kb	Ubiquitously expressed Mainly in various brain regions, aorta, lung, and thymus
	4.5kb and 2.5kb	Widely expressed No expression in liver
NCKX5*	10.5kb	Brain, eye, and thymus
	1.8kb	Eye and skin. Mouse melanoma cell line B16

* Data is based on the results from this study

Ca^{2+} can be substituted by Sr^{2+}, while Mg^{2+}, Ba^{2+}, and Mn^{2+} cannot be transported but will compete with Ca^{2+} to occupy the transport binding site (Schnetkamp 2004). Electrophysiology studies (Dong, Light et al. 2001) on NCKX2 expressed in transfected HEK293 cells revealed that the protein showed a $K_{1/2}$ for external Ca^{2+} of about 1μM or 100μM in the absence or presence of 1mM Mg^{2+} and a $K_{1/2}$ for external K^+ of about 12mM or 36mM with choline or Li^+ respectively and 30mM or 60mM for external Na^+ dependent activation or inhibition. Recently, Visser, F *et al*. (Visser, Valsecchi et al. 2006) reported that the apparent affinities for Ca^{2+} of NCKX3 and NCKX4 were similar to that of NCKX2 under the same conditions, with $K_{1/2}$ of 1.3-1.7μM, whereas the apparent affinities for K^+ of the two molecules were about 40-fold higher than that of NCKX2. NCKX3 and NCKX4 showed apparent $K_{1/2}$ values of 1.3mM and 1.1mM respectively for K^+. NCKX3 and NCKX4 also showed Na^+-dependent inactivation with IC_{50} values of 30mM and 18mM. It is also suggested in this work that NCKX2, 3, and 4 all have a single binding site for Ca^{2+} and K^+.

Mutagenesis studies on the key residues for ion binding in NCKX2 have also been conducted and some results are available. Several crucial residues thought to be involved in or to influence cation binding have been identified: Glu188, Asp548, Asp575 (Kang, Kinjo et al. 2005; Kang, Shibukawa et al. 2005; Kinjo, Kang et al. 2005), T551, and K558 (Visser, Valsecchi et al. 2006). Among them, Glu188 and Asp548, which are located in the α1 and the α2 repeats respectively, are suggested to be the key residues forming the K^+ and Ca^{2+} binding pocket (Kang, Kinjo et al. 2005; Kinjo, Kang et al. 2005). Asp575, located in the ninth transmembrane segment and conserved in all NCKX members at the corresponding position is thought to be the critical residue for K^+ binding

and transport as mutations in Asp575 of NCKX2 either abolishes the K^+-dependent property or generates non-functional protein (Kang, Shibukawa et al. 2005). T551A mutation in NCKX2 dramatically increases the K^+ affinity and K558Q mutation in NCKX2 results in decreased affinity for both K^+ and Ca^{2+}. As both of these residues lie near the cytoplasmic side of the membrane, it is most likely they influence cation binding indirectly, such as via conformational changes (Visser, Valsecchi et al. 2006).

Several regulatory effects of NCKX2 activity, i.e. PKC activation and Na^+-dependent inactivation, have been identified. It has been reported that NCKX2 activity increases in response to PKC activation whereas double mutations T166A/T476A and T476A/S504A disrupted the PKC induced enhancement of NCKX2 activity. However, the PKC-mediated activation was not observed in NCKX3 or NCKX4 (Lee, Visser et al. 2006). It also has been reported that high intracellular Na^+ concentration led to a large NCKX2-mediated increase in intracellular Ca^{2+} concentration and results in inactivation of NCKX2 activity. Two residues, Asp548 and Asn572, located in the α2 repeat and conserved in all NCX and NCKX members are thought to play a crucial role in this Na^+-dependent inactivation phenomenon since mutation of either of these two residues resulted in enhanced inactivation and higher affinity of NCKX2 for Na^+ (Altimimi and Schnetkamp 2007).

Knock-out (KO) mice were generated to study the function of NCKX2 in animals. The study (Li, Kiedrowski et al. 2006) revealed that NCKX2 KO mice had a significant decrease in Ca^{2+} flux in cortical neurons with loss of long-term potentiation and an increase in long-term depression. It was also reported in the same study that NCKX2 KO

mice showed very specific deficits in experience-dependent learning and memory which might have been due to the loss of control of local Ca^{2+} homeostasis in specific neuronal populations.

1.5 NCKX5

Earlier this century, a novel member in the NCKX subfamily, named NCKX5, was identified and reported by Japanese research groups working on the mouse genome project (Okazaki, Furuno et al. 2002). NCKX5 sequences of several species, such as mouse, human, and rat, have been deposited in the expressed sequence databases. The mouse NCKX5 gene maps to chromosome 2 and the whole gene spans more than 20kb on the chromosome. There are nine exons spreading over the 20kb region and the first two exons are about 10kb distant from the other seven (Figure 3). The coding region of mouse NCKX5 cDNA is about 1600 bp in length and the protein it encodes contains 501 amino acids.

The NCKX5 protein shares high amino acid identity and similarity with other NCKX family members in the two clusters of transmembrane-spanning segments but shows very little similarity in the two hydrophilic termini and cytoplasmic loop (Figure 2). The predicted topological structure of NCKX5 is similar to the other members of the NCKX family (Figure 1). It begins with a cluster of six hydrophobic transmembrane segments, the first of which may be cleaved during protein maturation because of the existence of a predicted signal peptide cleavage site, which would produce a mature protein with a calculated size of 52kDa. There is a predicted N-glycosylation site immediately after the signal peptide cleavage site, which suggests that the N-terminus

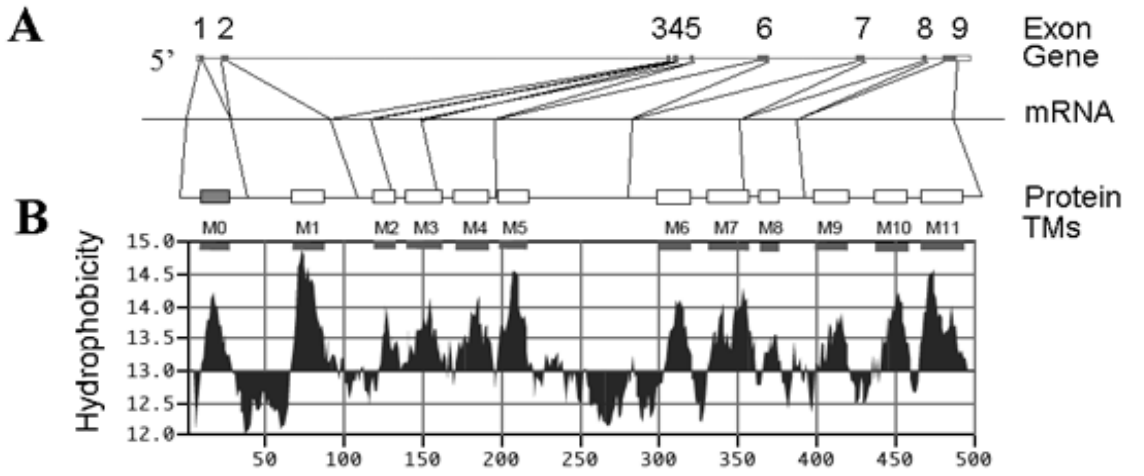

Figure 3. Exon organization and hydrophobicity profile of mouse NCKX5. A shows gene structure and exon organization of NCKX5. Gene, exons, mRNA, protein, and transmembrane segments are labeled correspondingly. Filled squares in the Gene row represent the coding regions of mouse NCKX5 while open squares in the same row represent the non-coding regions. Exons are labeled from 1 to 9. The squares in the Protein row represent the transmembrane-spanning segments. They are labeled from 0 to 11. **B** shows the hydrophobicity profile of mouse NCKX5 protein. The transmembrane-spanning segments are labeled from M0 to M11. Note that M6, although hydrophobic in nature, is not thought to span the membrane.

of the mature protein is on the extracellular side of the membrane. After the first cluster of transmembrane-spanning segments, there is a large hydrophilic loop at the cytosolic side followed by the second cluster of five transmembrane-spanning segments.

Although NCKX5 is the newest member found in NCKX family, some studies have already been done on it. In 2005, Cheng and colleagues reported some striking findings about NCKX5 (Lamason, Mohideen et al. 2005), which are unique to this gene product and quite different from other NCKX subfamily members. Using linkage analysis, shotgun sequencing, contig assembly, and gene knockdown techniques, Cheng's group found a truncation mutation in the zebrafish NCKX5 orthologue resulted in the *golden* phenotype, which is characterized by delayed and reduced development of melanin pigmentation. When full length zebrafish NCKX5 or human NCKX5 RNA was injected into *golden* zebrafish embryos, the *golden* phenotype could be partially rescued. Furthermore, it was reported in the same article that a polymorphism Ala111Thr in human NCKX5 has a strong association with the paler skin as well as lighter eye and hair color seen in Caucasian people. They further proposed that the human Thr111Ala polymorphism associated with light pigmentation has reduced function compared to the wild type form. It has also been reported that NCKX5 transcripts are most abundantly expressed in mouse melanoma cell line B16 and highly expressed in mouse eye as well as skin tissues. However, B16 cells show about 100-fold greater expression of NCKX5 compared with normal eye and skin. The NCKX5 expression level also varies greatly in different mouse tissues. Mouse eye and skin show over ten times greater expression of NCKX5 than other tissues. It has also been found that unlike all the other four members in the NCKX subfamily, NCKX5 is located inside the cells. As the truncation mutation in

NCKX5 causes *golden* phenotype in zebrafish, Cheng's group proposed that NCKX5 protein is localized on the membrane of the melanosome. A model including NCKX5, Na^+/H^+ exchanger, and vacuolar proton ATPase (V-type ATPase) was proposed by the same group to explain a possible way that NCKX5 works. The model suggested that V-type ATPase, Na^+/H^+ exchanger, and NCKX5 are coupled and V-type ATPase is the energy source of this transporting network. V-type ATPase transports proton into melanosomes by hydrolyzing ATP to keep the low pH environment at the luminal side of melanosomes, while Na^+/H^+ exchangers utilize the H^+ gradient generated by V-type ATPase to transport Na^+ into melanosomes. At the same time, NCKX5 uses the Na^+ gradient across the melanosome membrane to actively transport Ca^{2+} into melanosomes. However, the role that Ca^{2+} plays in melanosome maturation remains unclear. Moreover, no functional studies on NCKX5 have been undertaken. Nor is there any evidence for NCKX function or ion gradients required to drive Ca^{2+} uptake as proposed by these investigators. Later, several papers (Izagirre, Garcia et al. 2006; Norton, Kittles et al. 2006; Soejima and Koda 2007) from different research groups using human population genetic methods all confirmed that the NCKX5 gene has an association with the variations of human eye, hair, and especially skin color. Using proteomic, bioinfomatic, and molecular biology methods, Chi, A. *et al.* (Chi, Valencia et al. 2006) further demonstrated that the NCKX5 protein is a stage specific protein, which is only present in stage III and stage IV melanosomes.

1.6 Melanocyte, Melanin, and Melanosome Biogenesis

The melanocyte is a kind of specialized, highly dendritic cell located in the bottom layer of the skin's epidermis, inside hair bulbs, and in the retinal pigment epithelium (RPE) of the eye. Melanocytes produce the pigment proteins, melanin, inside specialized granules known as melanosomes (Marks and Seabra 2001; Hearing 2005).

Melanin, an insoluble tyrosine-based heteropolymer, is the major determinant of virtually all visible eye, hair and skin colors (Sharma, Wagh et al. 2002). In lower species, melanin pigmentations are important for thermoregulation, camouflage, and sexual attraction. In mammals' skin and hair, melanin protects the body against environmental challenges, such as UV exposure and heavy metals (Hearing 2005; Jackson 2006). In eyes, melanin enhances visual acuity by controlling light scatter (Marks and Seabra 2001). There are three types of melanin: the black-brown eumelanins, the yellow-reddish pheomelanins (Kongshoj, Thorleifsson et al. 2006), and the dark brown neuromelanins (Carstam, Brinck et al. 1991). Eumelanins consists of indolic units which are the products of hydroxylation, oxidation, and carboxylation of tyrosine. In contrast, pheomelanins are composed of benzothiazines which result from oxidation of cysteinyldopa units (Kongshoj, Thorleifsson et al. 2006). Neuromelanins, derived from the neurotransmitter dopamine, have the properties of both eumelanins and pheomelanins, containing both indole and benzothiazine units (Carstam, Brinck et al. 1991).

Melanosomes, a kind of membrane-bound lysosome-related subcellular organelle that is generated in melanocytes, are the place within which melanin pigments are synthesized and stored (Dell'Angelica 2003). Since the melanosome is a kind of

lysosome-related organelle, it shares some common features with lysosomes, such as a low intraluminal pH environment and lysosomal hydrolases (Dell'Angelica, Mullins et al. 2000). It also shares some proteins and protein sorting pathways with other lysosome-related organelles (Dell'Angelica, Mullins et al. 2000), but there are some specific melanosomal proteins that exist only in melanosomes, exemplified by the tyrosinase gene family proteins (Jimbow, Park et al. 2000).

The concept of melanosome biogenesis was proposed in 1960s and it remains essentially valid today (Jimbow, Park et al. 2000; Hearing 2005). Melanosome development can be classified into four stages (stage I to IV) according to their different morphologies and the involvement of different proteins (Dell'Angelica 2003). Some of the proteins participating in melanosome maturation have been identified, cloned and studied (Kushimoto, Basrur et al. 2001). These proteins fall into three distinct categories: enzymatic proteins, such as tyrosine, tyrosinase-related protein 1 (TYRP-1), and dopachrome tautomerase (DCT); structural proteins, like Pmel 17; and proteins of unknown functions, like MART1 and OA1 (Hearing 2005). All of the known melanosomal proteins are glycosylated (Hearing 2005), have unique signature sequences helping them to target to the correct stages of melanosomes (Jimbow, Park et al. 2000), and may have some modifications to help them stabilize in the acidic environment (Marks and Seabra 2001).

The generation of the stage I melanosome, which is also termed premelanosome, remains controversial. Some studies suggested that the stage I melanosomes were amorphous or spherical shape vesicles that budded directly from the ER (Hearing 2005),

while others proposed that the stage I melanosomes arose from late endosomes (Kushimoto, Basrur et al. 2001). Despite the uncertainties in the origin of the stage I melanosome, it is commonly recognized that the Pmel 17 protein, also known as gp100 or *silver* locus protein, is delivered to the stage I melanosomes and plays a key role in the formation of the characteristic striated structures. which marks the transition of the melanosomes from stage I to stage II (Dell'Angelica 2003). The sorting signal at the N-terminus of the Pmel 17 protein leads it to the ER immediately after synthesis (Hearing 2005). Within the ER, it is modified with high-mannose oligosaccharides and then it is translocated into the *trans*-Golgi network (TGN). Through TGN, Pmel 17 is further glycosylated and the C-terminus of the protein is cleaved (Dell'Angelica 2003). The remaining N-terminal portion is then transported to the premelanosomes in which it forms striated structures which provide a scaffold for the precipitation, binding, and polymerization of melanin synthesized in later stages (Kobayashi, Urabe et al. 1994). The adaptor protein 3 (AP-3) is thought to facilitate the targeting of Pmel 17 to premelanosomes (Marks and Seabra 2001). Along with the advent of the striated structures, the shape of the premelanosome transforms from spherical to elongated oval. The melanosomes enter the second stage (Hearing 2005).

The well known proteins involved in stage II melanosomes are tyrosinase gene family proteins which include tyrosinase, tyrosinase-related protein 1 (TYRP-1), and dopachrome tautomerase (DCT, also known as TYRP-2) (Jimbow, Park et al. 2000). The sorting of these catalytic proteins to melanosomes is another significant sign of stage II melanosoms (Hearing 2005). Some ancillary proteins, such as AP-3 (Hearing 2005) and calnexin (Jimbow, Park et al. 2000), are also required for the transport and sorting of

tyrosinase gene family proteins. Like Pmel 17, the proteins in the tyrosinase gene family all have sorting signals leading them to the ER after synthesis. First glycosylated in the ER, they are translocated into TGN to be further glycosylated and processed (Hearing 2005). Calnexin, which is a Ca^{2+} binding phosphoprotein, is essential for the translocation of the tyrosinase gene family proteins from the ER to the TGN. Calnexin, functioning as a molecular chaperone, associates with unassembled or incompletely folded glycoproteins to facilitate them acquiring the correct three-dimensional structures and translocating to the TGN (Jimbow, Park et al. 2000). The mature tyrosinase and TYRPs leave the TGN in coated or non-coated vesicles derived from the TGN (Marks and Seabra 2001). These tyrosinase carrying vesicles are sorted to and fused with premelanosomes, and transfer the tyrosinase/calnexin complexes into the stage I melanosomes (Jimbow, Park et al. 2000). This sorting process requires the involvement of AP-3. AP-3 recognizes the signature sequence EEXXXLL at the cytoplasmic tail of the tyrosinase and binds to it (Honing, Sandoval et al. 1998) to facilitates its correct target and delivery (Jimbow, Park et al. 2000).

In stage III melanosomes, melanin synthesis begins and the pigment is deposited uniformly on the striated structures within melanosomes. Tyrosinase gene family proteins, which were sorted into melanosomes at stage II, play an essential role in the process of melanin synthesis (Marks and Seabra 2001). Tyrosinase can use tyrosine, 3,4-dihydroxyphenylalanine (DOPA), and 5,6-dihydroxyindole-melanin (DHI) as substrates (Jimbow, Park et al. 2000). But in melanin synthesis, the hydroxylation of tyrosine is the rate-limiting step (Kushimoto, Basrur et al. 2001). Tyrosinase hydroxylates tyrosine to produce DOPAquinone which then rapidly cyclizes, decarboxylates, and polymerizes to

form DHI-melanin, a very black, insoluble, and high molecular weight pigment. To synthesize DHICA-melanin, which is a more soluble, lower molecular weight, and lighter colored melanin, DCT is needed. In the presence of DCT, the carboxylic acid group of DOPAchrome is maintained, thus a carboxylated intermediate (DHICA) but not the DHI is produced, which leads to a much slower process of further oxidation and polymerization (Sharma, Wagh et al. 2002; Hearing 2005).

With more melanin synthesized and deposited, the melanosomes enter the fourth stage, at which point no structural detail can be visualized within them (Dell'Angelica 2003). The fully matured and highly pigmented melanosomes are transported to the dendrites of melanocytes mainly relying on the function of F-actin, myosin (Hearing 2005), and microtubules (Marks and Seabra 2001). When these mature melanosomes reach the periphery of the melanocytes, they are released from the microtubules (Marks and Seabra 2001) and bind to nearby actin filaments, on which they undergo local short-range movements (Marks and Seabra 2001; Hearing 2005). Mature melanosomes are evenly distributed at the periphery of melanocytes (Marks and Seabra 2001) from where they are further transferred to neighboring keratinocytes (Hearing 2005). There are three models proposed for the melanosome transfer process (Marks and Seabra 2001). The first is a direct membrane fusion model which suggested that the melanocyte fuses with the adjacent keratinocyte and thus a passageway is formed for melanosome translocation. The second model involves phagocytosis of the dendrites of melanocytes by basal keratinocytes. The third model suggests the exocytosis of melanosoms from the dendrites of melanocytes and endocytosis by keratinocytes. However, the detailed molecular mechanisms of melanosome transfer are still poorly understood (Hearing 2005).

In many pigmented cells, melanosomes are known to contain Ca^{2+} deposits and serve as a Ca^{2+} reservoir (Salceda and Sanchez-Chavez 2000). It has been reported that pigment granules of the RPE contain high Ca^{2+} concentration (Hess 1975), and that the concentration is 7-10 fold higher in pigmented mammals than in albino (Drager 1985). High Ca^{2+} concentration has also been reported in other pigmented eye tissues, such as iris and choroids (Panessa and Zadunaisky 1981). A strong correlation between Ca^{2+} accumulation and melanin content in chick RPE of different degrees has been reported (Salceda and Riesgo-Escovar 1990), which indicates that Ca^{2+} might be involved in the regulation of melanosome mobility (Salceda and Sanchez-Chavez 2000).

1.7 Study objectives

Although some recent studies have been conducted on NCKX5, almost nothing is known about the biochemical or physiological role of NCKX5. It is notable that although NCKX5 has been shown to be involved in the pigmentation process, there is almost no information regarding the role of Ca^{2+} or the NCKX5 protein in the processes of melanosome maturation and melanin synthesis. To characterize mouse NCKX5 at the molecular level, four objectives were proposed and examined in this research project.

The first objective was to determine the mRNA expression level and tissue distribution pattern of mouse NCKX5 transcripts in a series of mouse tissues by Northern blotting.

The second objective was to express mouse NCKX5 constructs in HEK293 cells and detect the expression of recombinant NCKX5 protein by immunoblot. Moreover,

detection of the endogenous NCKX5 protein expression in melanoma cell lines was also included in this study aim.

The third objective was to study the subcellular localization of NCKX5 protein both in HEK293 cells and in melanoma cell lines.

The last objective was to study the transport function of NCKX5 protein using Ca^{2+}-sensitive assays.

The findings from these studies will help us gain more knowledge about the biochemical and molecular properties of NCKX5. They may also shed some light on the roles that Ca^{2+} and NCKX5 play during melanosome biogenesis maturation and the process of pigmentation in mammals.

CHAPTER TWO

MATERIALS AND EXPERIMENTAL PROCEDURES

2.1 Materials, Chemicals and Reagents

Common chemicals reagents were purchased from Fisher, Sigma, or BDH and were of the highest available molecular biology grade. All the restriction enzymes were purchased from New England Biolabs. Molecular cloning procedures were conducted essentially following published standard protocols (Ausubel 2001; Sambrook 2001) or those provided by the reagent suppliers unless indicated otherwise. Fluorescent dye terminator cycle sequencing and DNA primer synthesis were done at the University of Calgary Core DNA Services Facility.

2.2 Experimental Procedures

2.2.1 Subcloning of mouse NCKX5

Reverse transcription-coupled polymerase chain reaction (RT-PCR) amplification was employed to obtain the NCKX5 clone from mouse brain, kidney and B16 cell total RNA (prepared as described in p36, a generous gift from Dr. Xiao-Fang Li). Briefly, 5µg of ethanol precipitated total RNA was centrifuged, washed, dried and dissolved in 7µl of RNA-grade H_2O by heating at 65°C for 5 minutes, and then quickly cooled on ice. 4µl of 5X first strand buffer, 2µl of 0.1M DTT, 1µl of 10mM mixed dNTPs, and 1µl of 0.5mg/ml oligo$(dT)_{12\text{-}18}$ were added and the mixture was pre-warmed at 42°C for 2 minutes. 5µl of Superscript II (200U/µl) was then added and the mixture was incubated at

42°C for 1 hour. The mixture was finally heated at 95°C for 5 minutes to stop the reaction.

2μl of the above first strand DNA was used as template to start the PCR reaction. A pair of specific primers (Mus NK5-F: *GGA ATT CC*C AAA GAG CAC GCT GGA AAT G and Mus NK5-R: *GGA ATT CC*T TCC ATC TTT CCA CAT AAC ACT), based on the mouse NCKX5 sequence AK_089225 and located flanking the start and stop codons (shown as underlined) of the reading frame, each with an EcoRI linker (shown in Italic), was used to amplify the coding region of mouse NCKX5. The RT-PCR product from B16 total RNA was sequenced directly using Mus NK5-3, Mus NK5-4, and Mus NK5-R primers (Table 2). The RT-PCR products from mouse brain and kidney total RNA were gel purified and digested with EcoRI. The digested segment was inserted into the EcoRI site of vector pBlueScript II SK (-). Electroporation was used to transform the NCKX5 carrying vector into DH10B competent cells (Invitrogen). Single colonies were picked up and cultured. Minipreps were done using QIAprep Spin Miniprep Kit (QIAGEN) and pure mouse NCKX5 clones were obtained. Restriction digestion was performed to confirm the existence of the insert. The clone was finally sequenced to ensure its accuracy.

2.2.2 Epitope insertion and expression constructs

The overlapping PCR technique was used to insert FLAG or HA epitope into different positions of mouse NCKX5 clone (Figure 4 and 6). FLAG epitope was inserted separately at the N-terminus, C-terminus, as well as in the cytoplasmic loop region, and the HA epitope was inserted separately into the same positions as the FLAG epitope at

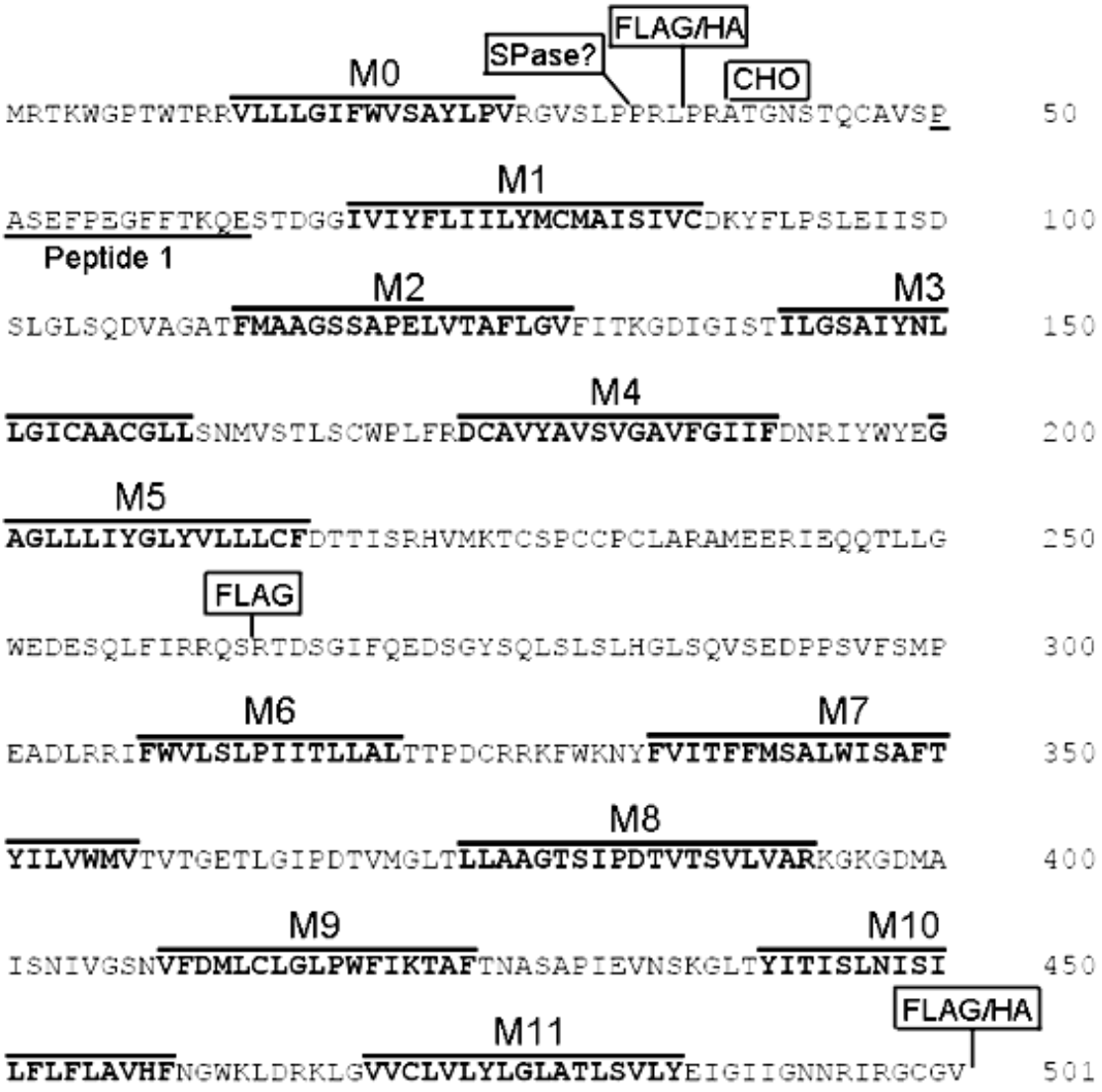

Figure 4. Amino acid sequence of mouse NCKX5. The transmembrane segments are indicated as M0 to M11 (M6 is actually proposed not to cross the membrane); FLAG/HA indicates the position where the epitope was inserted; SPase? indicates the proposed signal peptidase cleavage site; CHO indicates the proposed N-glycosylation site; Peptide 1 indicates the antigen region used for raising anti-NCKX5 serum.

the N-terminus and C-terminus of mouse NCKX5. A series of specific primers (Table 2) were used to insert the epitope into those positions.

To insert the epitope into the C-terminus of NCKX5, C-FLAG-R or C-HA-R primer paired with Mus NK5-F primer were used. As these reverse primers contain the whole FLAG or HA sequence, one round of PCR was performed to insert the epitope into the end of the NCKX5 clone, immediately before the stop codon. To insert the FLAG epitope into the cytoplasmic loop, L-FLAG-F primer paired with Mus NK5-R primer was used to amplify the first 789bp of NCKX5 and part of the epitope. L-FLAG-R primer paired with Mus NK-5-F primer was used to amplify the last 714bp of NCKX5 and part of the epitope, which has 21bp overlapping with the first part. The second round PCR was performed with a mixture of the first two products as templates using the Mus NK5-F and Mus NK5-R primer pair to amplify the whole NCKX5 coding sequence with the FLAG epitope inserted into the cytoplasmic loop. These PCR products were first digested with EcoRI and cloned into the EcoRI site of pBlueScript II SK (-). Individual clones were obtained by electroporation and minipreps. Then, these tagged clones together with the wild type NCKX5 clone were digested with HindIII and NotI and cloned into the HindIII and NotI sites of the mammalian expression vector pcDNA3.1(+). Electroporation was done to transform these NCKX5 carrying vectors into DH10B cells individually. Single colonies were picked up and cultured. First, minipreps were prepared to get pure clones. Next, these clones were sequenced to ensure that they were free of mutations.

To obtain N-terminal tagged NCKX5, the wild type NCKX5 clone in pBlueScript II SK (-) was first digested with HindIII and NotI and about 700bp of the latter half of the

Table 2. Primers for NCKX5 amplification, epitope insertion, and Northern blot DNA probe amplification

Primer	Sequence
Mus NK5-F	5'-*GGA ATT CC*C AAA GAG CAC GCT GGA AAT G
Mus NK5-R	5'-*GGA ATT CC*T TCC ATC TTT CCA CAT AAC ACT
Mus NK5-3	5'-GAA GAT TCC GGT TAC TCC C
Mus NK5-4	5'-CTG AAA ACA CTT GGT GGA TCT
N-tag-F	5'-CGT AAT ACG ACT CAC TAT AGG
N-FLAG-F	5'-**TAC AAG GAC GAC GAT GAC AAG** CCA AGG GCC ACA GGA AAC
N-FLAG-R	5'-**GTC ATC GTC GTC CTT GTA GTC** GAG GCG CGG GGG CAG
N-HA-F	5'-**CCA TAT GAT GTC CCT GAC TAT GCC** CCA AGG GCC ACA GGA AAC
N-HA-R	5'-**ATA GTC AGG CAC ATC ATA TGG GTA** GAG GCG CGG GGG CAG
C-FLAG-R	5'-*CGG AAT TCC G*TC A**CT TGT CAT CGT CGT CCT TGT AGT C**AA CTC CAC AAC CCC TTA TTC T
C-HA-R	5'-*CGG AAT TCC G*TC A**GG CAT AGT CAG GCA CAT CAT ATG GGT A**AA CTC CAC AAC CCC TTA TTC T
L-FLAG-F	5'-**TAC AAG GAC GAC GAT GAC AAG** AGG ACA GAC AGT GGA ATA TTT
L-FLAG-R	5'-**GTC ATC GTC GTC CTT GTA GTC** TGA CTG GCG ACG AAT GAA GA
MS-N5-5F	5'-CAA AGA GCA CGC TGG AAA TGC
MS-N5-5R	5'-CTC CTG CTT GGT GAA GAA CCC
M-F-L	5'-CTG TCC AAC ATG GTT TCA ACA C
M-R-L	5'-GTG CAG ACA TGA AAA AGG TTA TC

Start and stop codons are underlined. Linkers containing restriction digestion site are shown in italic. Epitope sequences are shown in bold.

NCKX5 region bounded by these restriction sites was inserted into pcDNA3.1(+) digested with the same enzymes. Electroporation and miniprep were performed to obtain the desired DNA construct named NCKX5-L. Second, two primer pairs, N-tag-F paired with N-FLAG-R or N-HA-R, and N-FLAG-F or N-HA-F paired with Mus NK5-4, were used in the first round of PCR with the wild type NCKX5 clone as templates. As the N-tag-F primer is around 80bp upstream of the start codon of the NCKX5 clone in pBlueScript II SK (-), the first primer pair amplified part of the vector including a HindIII site, the first 125bp of NCKX5, and part of the epitope. The second primer pair was used to amplify the following 785bp of NCKX5 and part of the epitope which has 21bp (FLAG) or 24bp (HA) overlapping with the epitope in the first half. N-tag-F/Mus NK5-4 primer pair was used for the second round PCR with a mixture of the above PCR products to amplify the first 900bp of NCKX5 including the epitope inserted at the N-terminus. The final PCR product was digested with HindIII and cloned into the HindIII site of NCKX5-L. Electroporation was done to transform these NCKX5 carrying vectors into DH10B cells. Single colonies were picked up and cultured. Minipreps were prepared to get pure clones. Next, restriction digestion was done to ensure the insert with both HindIII ends was in the correct orientation. The clones with the correct insert orientation were sequenced to ensure that they were free of mutations.

Finally, maxipreps were done on all these constructs using the HiSpeed QiaSpin Kit (QIAGEN) according to the manufacturer's instruction to obtain high quality and desired concentration of DNA solutions which were suitable for transfection.

2.2.3 RNA Extraction

One gram of mouse tissue was placed into a 50ml polystyrene conical bottom tube containing 7.5ml GITC buffer (4M guanidinium isothiocyanate, 25mM sodium citrate, and 0.7% β-mercaptoethanol) and homogenized using a Polytron on maximum speed for two 15-second bursts. 375µl of 10% Na-lauryl sarcosine (Sarkosyl) was added to the homogenate. The homogenate was transferred to an uncapped Falcon 1059 tube and centrifuged at 12,000g, 15°C for 10 minutes. The supernatant was layered over 4ml of CsCl/NaAcetate cushion (5.7M CsCl, and 25mM sodium acetate) in an SW41 ultracentrifuge rotor tube and subjected to a 32,000rpm centrifugation at 18°C overnight. The next day, the supernatant was aspirated and the pellet was rinsed twice with 75% ethanol and air dried. The dry pellet was resuspended in 400µl RNA-grade H_2O, vortexed well, heated at 65°C for 10 minutes so that the RNA was completely dissolved, and then quickly cooled on ice. Finally, 40µl of 3M sodium acetate and 1ml of ice-cold 100% ethanol were added, mixed well and the precipitated RNA sample was stored in -80°C.

2.2.4 Northern blot analysis

2.2.4.1 Probe Preparation

Two pairs of specific PCR primers, MS-N5-5F/MS-N5-5R and M-F-L/M-R-L (Table 2), were synthesized. The first pair is for the amplification of the 5'-end of mouse NCKX5 (from nucleotide 42 to 247, Figure 6) and the second pair is for the amplification of the whole cytoplasmic loop (from nucleotide 535 to 1088, Figure 6). Mouse NCKX5 clone was used as a template and PCR was conducted to amplify the corresponding

regions in the clone. The PCR products were separated on a 1% agarose gel and the DNA segments were extracted and purified using a Gel Extraction Kit (QIAGEN) according to the manufacturer's instruction. The purified DNA segments were then labeled with DIG DNA labeling Mix (Roche) according to the manufacturer's instruction as probes for next step.

2.2.4.2 Northern blot

Ten micrograms of ethanol-precipitated mouse total RNA was centrifuged, washed, dried, dissolved in 2.5µl of RNA-grade H_2O by vortex mixing, heated for 5 minutes at 65°C, and quickly cooled on ice. 13.5µl of freshly made loading buffer (50% formamide, 10% 10X MOPS buffer, 20% of 37% formaldehyde, 10% "dye mix", 9% RNA-grade H_2O, and 1% of 10 mg/ml ethidium bromide stock solution) was added to each sample. Next, the samples were loaded and separated on 1% RNA agarose-formaldehyde gel (0.5g agarose, 5ml of 10X MOPS buffer, 2.55ml of 37% formaldehyde, and 42.5ml of RNA-grade H_2O) at 60V for about 2.5 hours to achieve good separation. Then the RNA samples on the gel were transferred to a nylon membrane by capillary diffusion in 10X SSCP solution (1.2M NaCl, 150mM NaCitrate, 130mM KH_2PO_4, and 10mM EDTA, pH7.2) overnight at room temperature.

The next day, the transfer "sandwich" was disassembled and the RNA was UV cross-linked into place. The UV-cross-linked membrane was first pre-hybridized in hybridization solution (50% formamide, 5X SSCP, 0.1 % N-lauroyl sarcosine, 2% SDS, and 5% "blocking reagent", which is from Boehringer-Mannheim) at 50°C for 1 hour. The probe was heated at 85°C for 3 minutes, quenched on ice, and then diluted in the

hybridization solution to a final concentration of 25ng/ml. The membrane was hybridized at 50°C overnight.

The third day, the membrane was first washed several minutes with 2X SSCP plus 0.1% SDS at room temperature and then washed twice, for 15 minutes each wash, with 2X SSCP plus 0.1% SDS at 50°C, and later washed twice, again for 15 minutes each wash, with 0.1X SSCP plus 0.1% SDS at 50°C. After hybridization and the aforementioned high stringency washes, the membrane was rinsed briefly in washing buffer, whose components are maleic acid buffer (0.1M maleic acid and 0.15M NaCl, pH 7.5) with 0.2% Tween20, and incubated for half an hour in 1X blocking buffer (10X blocking buffer is 10g blocking agent dissolved in 100ml maleic acid buffer plus 100µl of DEPC; this is diluted 1:10 with maleic acid buffer to generate 1X blocking buffer). Anti-DIG-AP antibody was diluted 1:20,000 into the blocking buffer and the membrane was incubated for another half an hour. Then the membrane was washed twice in washing buffer, for 15 minutes each wash, and equilibrated briefly in detection buffer (0.1M Tris-HCl, 0.1M NaCl, and 50mM $MgCl_2$, pH 9.5). The signal was detected using CDP-Star (Roche) following the manufacturer's instruction. The probe preparation and Northern blot experiment were performed by Dr. Xiao-Fang Li.

2.2.5 Cell culture and transfection

2.2.5.1 Culturing HEK293 cells

HEK293 cells were used as the expression system to produce recombinant NCKX5 protein. HEK293 cells were maintained in a 37°C cell culture incubator under 5% CO_2 in high glucose Dulbecco's modified Eagle's medium (DMEM) which was supplemented

with 2mM L-glutamine, 1% MEM non-essential amino acids (NEAA), 10% fetal bovine serum (FBS), 100units/ml penicillin, and 100μg/ml streptomycin. Cells were split prior to confluence twice per week.

2.2.5.2 HEK293 cell transfection

Cells at 40%-50% confluence in 100mm dishes were transfected using a standard calcium phosphate precipitation protocol. Briefly, 20μl of 0.5mg/ml DNA was mixed with 430μl of H_2O and 50μl of 2.5M $CaCl_2$. This solution was then added dropwise to 0.5ml of 2X BES, which contained 280mM NaCl, 50mM BES, 1.5mM Na_2HPO_4, pH 7.0. At the same time, a pipetting-aid was used to provide a steady stream of bubbles from the bottom of the tube for good mixing. After 5 minutes, the solution became a little cloudy, due to the precipitation of calcium phosphate. One ml of the cloudy solution was added dropwise to each plate. The plates were then swirled gently and returned to the incubator.

2.2.5.3 Culturing melanoma cell lines

Mouse melanoma cell line B16 and human melanoma cell line MNT1 (a generous gift from Dr. Victor A. Canfield, Dept. of Pharmacology, The Pennsylvania State University College of Medicine) were used to study the endogenous NCKX5 protein. Both of the cell lines were maintained in a 37°C cell culture incubator under 5% CO_2. B16 cells were cultured in high glucose DMEM with reduced sodium bicarbonate (1.5g/L) supplemented with 2mM L-glutamine, 1% MEM NEAA, 10% FBS, 100units/ml penicillin, and 100μg/ml streptomycin. B16 is a fast-growing cell line, which was usually passaged twice a week with 1:50 dilution. MNT1 cells were cultured in high glucose DMEM supplemented with 2mM L-glutamine, 1% MEM NEAA, 20% FBS, 10% AIM-V

medium, 20mM Hepes, 1mM sodium pyruvate, 100units/ml penicillin, and 100µg/ml streptomycin. MNT1 is a slow-growing cell line, which was passaged twice a week with 1:5 dilution. Both cell lines require Trypsin/EDTA to be detached from the culture flasks when passaging them.

2.2.6 Protein preparation

2.2.6.1 Post nuclear preparation

Two days after transfection for HEK293 cells or at confluence for B16 and MNT1 cells, one 100mm cell culture dish was first rinsed twice with 1X PBS (140mM NaCl, 2.7mM KCl, 10mM Na_2HPO_4, 1.8mM KH_2PO_4, pH 7.4) and then 2ml of 1X PBS/5mM EDTA was added to each plate. Cells were harvested using a cell scraper and transferred to a 15ml polystyrene conical bottom tube. The cell suspension was centrifuged at 1,500 rpm, 4°C for 3 minutes in a clinical centrifuge. The supernatant was aspirated and the pellet was re-suspended in 1ml of 1X PBS/5mM EDTA. The suspension was transferred to a 1.7ml microcentrifuge tube and centrifuged again at 5,000 rpm, 4°C for 1 minute in a benchtop microcentrifuge. The supernatant was aspirated and the pellet was suspended in 100µl of RIPA buffer (25mM Tris-HCl pH7.5, 10mM EDTA, 140mM NaCl, 1% Triton-X100, 0.1mM PMSF, and 100U/ml aprotinin) and incubated on ice for 20 minutes. The suspension was finally centrifuged at 16,200g, 4°C for 5 minutes in a benchtop microcentrifuge. The supernatant was transferred to a fresh 1.7ml microcentrifuge tube and stored in -80°C.

2.2.6.2 Membrane preparation

This preparation procedure is revised from previously published work (Maruyama and MacLennan 1988). Two days after transfection for HEK293 cells or at confluence for B16 and MNT1 cells, five 100mm cell culture dishes were first rinsed twice with cold 1X PBS and then 2ml of cold 1X PBS/5mM EDTA was added to each plate. Cells were harvested using a cell scraper and transferred to a 15ml polystyrene conical bottom tube. The cell suspension was centrifuged at 1,500 rpm, 4°C for 3 minutes in a clinical centrifuge. The supernatant was discarded and the pellet was re-suspended in 5ml of 1X PBS. The suspension was centrifuged again at 1,500 rpm, 4°C for 3 minutes in a clinical centrifuge. Supernatant was aspirated and the pellet was suspended in 2ml of LIS buffer (10mM Tris-HCl pH7.5, and 0.5mM $MgCl_2$). The suspension was incubated on ice for about 10 minutes and aprotinin and PMSF were added to the suspension at the working concentration of 100unit/ml and 1mM, respectively. The suspension was homogenized 40 strokes in a 7ml Dounce with a tight A pestle. Two ml of solution A (0.5M sucrose, 10mM Tris-HCl pH7.5, 6mM β-mercaptoethanol, and 0.32M NaCl) was then added and 20 more strokes were done. The homogenate was transferred to a centrifuge tube fitting into JA20 rotor and centrifuged at 8,000g, 4°C for 20 minutes. The supernatant from 8,000rpm spin was transferred to a Ti75 polycarbonate tube to which 0.9 ml of 2.5M NaCl was previously added. The mixture was centrifuged at 100,000g, 4°C for 1 hour. The supernatant was removed and the pellet was carefully suspended in 100μl of solution B (0.25M sucrose, 5mM Tris-HCl pH7.5, 3mM β-mercaptoethanol, and 0.16M NaCl). The suspension was triturated and vortexed until no big particles were visible and

aliquoted into several microcentrifuge tubes. These aliquots were quickly frozen in liquid nitrogen and stored at -80°C.

2.2.6.3 Protein concentration measurement

Protein concentrations of both preparations were determined by the dye-binding Bradford assay using bovine γ-globulin as a standard with the protein assay kit from Bio-Rad.

2.2.7 Anti-NCKX5 antibody preparation

Anti-NCKX5 serum was prepared at Global Peptide Services (Fort Collins, CO) by immunizing New Zealand rabbits with a carrier-conjugated synthetic peptide corresponding to the sequence PASEFPEGFFTKQE (peptide 1; amino acid residues 50-63), which is located at the N-terminus, right before the first transmembrane segment, of the mouse NCKX5 protein (Figure 4).

As a cysteine residue was added to one end of the peptide, the anti-NCKX5 serum was affinity purified using Sulfolink Kit (Pierce) and the purified antibody was eluted from the column by 3.5M $MgCl_2$. The antibody purification work was done by Yiqian Wang, the technician in our laboratory.

In order to obtain a negative control for the anti-NCKX5 serum in both immunoblot and immunostaining, a peptide pre-absorption strategy was employed. Briefly, 10µl of anti-NCKX5 serum was mixed with 10µl of 1mg/ml of the peptide solution. The mixture was incubated at room temperature for 1 hour prior to use.

2.2.8 Immunoblot analysis

20μg of each protein sample pre-mixed with 4X Laemmli sample buffer (0.26M Tris-HCl pH 6.8, 8% SDS, 40% glycerol, and 5% Bromophenol Blue) was loaded and separated on 9% SDS-polyacrylamide gels. After electrophoresis, the gel was electrophoretically transferred to a nitrocellulose membrane.

The membrane was first blocked in 5% milk/PBS-T (1X PBS containing 0.1% Tween 20) for half an hour and then incubated with 1X PBS-T containing diluted primary antibody at room temperature for 1 hour and washed three times, for 5 minutes each wash, with 1X PBS-T. Then the membrane was incubated with 1X PBS-T containing diluted horseradish peroxidase-conjugated secondary antibody at room temperature for half an hour and washed three times, again for 5 minutes each wash, with 1X PBS-T. Enhanced chemiluminescence (Pierce Supersignal substrates, from Pierce) was used to detect the signal following the manufacturer's instruction.

NCKX5 protein expression was detected using either rabbit anti-NCKX5 serum (1:500) or affinity purified rabbit polyclonal anti-NCKX5 antibody (1:20). NCX1 protein expression was detected using mouse polyclonal anti-NCX1 antibody R3F1 (prepared by Taconic Labs, NJ) (1:10,000) (Porzig, Li et al. 1993). NCKX2 protein expression was detected using mouse anti-FLAG antibody (Sigma) (1:10,000) as the NCKX2 construct is FLAG tagged, or anti-NCKX2 F antibody (prepared in the Lytton Lab with assistance from the Faculty of Medicine Antibody Facility) (1:8,000) (Cai, Zhang et al. 2002). Mouse anti-FLAG antibody or mouse anti-HA antibody (Sigma) was also used to try and detect the expression of FLAG or HA tagged NCKX5. Peptide pre-absorbed anti-NCKX5

serum or antibody was used as a negative control in the native NCKX5 protein expression detection in B16 and MNT1 cells.

2.2.9 N-glycosidase F digestion

Post nuclear preparations or membrane vesicle preparations from B16 or MNT1 cells, or from HEK293 cells transfected with wild type NCKX5 or the three forms of FLAG tagged NCKX5, were used. Briefly, 40µg of the preparations were mixed with 15µl of 4X reaction buffer (50mM sodium phosphate, 10mM EDTA, 1% NP40, 0.1% SDS, and 1% β-mercaptoethanel) and 6µl of 1% SDS and H_2O was added to bring the total volume to 54µl. Then the mixture was equally divided into two fresh 1.7ml microcentrifuge tubes. For the reaction group, 3µl of N-glycosidase F (1U/µl) was added to each tube whereas 3µl of H_2O was added to tubes belonging to the control group. The two groups of tubes were incubated at 37°C for 2 hours and then they were mixed with the same volume (30µl) of 4X laemmli sample buffer and analyzed by immunoblot.

2.2.10 Immunostaining

HEK293 cells growing on poly-D lysine coated coverslips in 6-well dishes were transfected with either wild type NCKX5 construct or vector control, pcDNA3.1(+), using a standard Ca^{2+} phosphate protocol. Two days after transfection, the medium was aspirated, and the coverslips were rinsed once with 1X PBS/5mM $CaCl_2$ and $MgCl_2$. The cells were then fixed onto the coverslips by incubating them in 1ml per well of 3% paraformaldehyde in 1X PBS/5mM $CaCl_2$ and $MgCl_2$ for 20 minutes at room temperature. After fixation, the coverslips were washed twice with 1X PBS/5mM $MgCl_2$ and $CaCl_2$ and the cells were permeablized with 1xPBS/5mM $MgCl_2$ and $CaCl_2$ plus 0.1% Triton X-

100 for 20 minutes at room temperature. For non-permeablized controls, the above permeablization step was simply omitted. Then the coverslips were washed twice with 1X PBS/5mM $MgCl_2$ and $CaCl_2$ again and the cells were blocked in 0.2% fish gelatin in 1X PBS/5mM $CaCl_2$ and $MgCl_2$ for 20 minutes. After the fixing, permeablizing, and blocking steps, the cells were incubated with either 1X PBS/5mM $CaCl_2$ and $MgCl_2$ containing anti-NCKX5 serum (1:500 dilution) or 1X PBS/5mM $CaCl_2$ and $MgCl_2$ containing peptide pre-absorbed anti-NCKX5 serum (1:500 dilution) for 2 hours by inverting the coverslip onto a drop of diluted antibody on a piece of parafilm. Then the coverslips were washed 3 times, for 5 minutes each wash, with 1X PBS/5mM $CaCl_2$ and $MgCl_2$. The cells were incubated with 1X PBS/5mM $CaCl_2$ and $MgCl_2$ containing Cy3 or FITC conjugated anti-rabbit secondary antibody (1:800-1:1,000 dilution) for 1 hour in the same way as the primary antibody incubation and washed 3 times, for 5 minutes each wash, with 1X PBS/5mM $CaCl_2$ and $MgCl_2$. Finally, the coverslips were mounted upside-down onto slides and observed by fluorescent microscopy.

Immunostaining for B16 cells was virtually the same as transfected HEK293 cells. Briefly, B16 cells cultured on poly-D lysine coated coverslips at 70%-80% confluence were fixed and permeablized using an ice cold mixture of 70% methanol and 30% acetone for 20 minutes. The coverslips were washed twice with 1X PBS/5mM $CaCl_2$ and $MgCl_2$ and the cells were blocked using 0.2% fish gelatin in 1X PBS/5mM $CaCl_2$ and $MgCl_2$ for 20 minutes. Then the cells were incubated with either 1X PBS/5mM $CaCl_2$ and $MgCl_2$ containing affinity purified anti-NCKX5 antibody (1:10 dilution) or 1X PBS/5mM $CaCl_2$ and $MgCl_2$ containing peptide pre-absorbed affinity purified anti-NCKX5 antibody (1:10 dilution) for 2 hours by inverting the coverslip onto a drop of

diluted antibody on a piece of parafilm. The coverslips were washed 3 times, for 5 minutes each wash, with 1X PBS/5mM $CaCl_2$ and $MgCl_2$. Then the cells were incubated with 1X PBS/5mM $CaCl_2$ and $MgCl_2$ containing Cy3 or FITC conjugated anti-rabbit secondary antibody (Jackson Labs) (1:800-1:1,000 dilution) for 1 hour in the same way as primary antibody incubation and washed 3 times, for 5 minutes each wash, with 1X PBS/5mM $CaCl_2$ and $MgCl_2$. Finally, the coverslips were mounted upside-down onto slides and observed by fluorescent microscopy. The NCKX5 staining in B16 cells was performed by Yiqian Wang.

2.2.11 Function assay

2.2.11.1 Ca^{2+} uptake into membrane vesicles

The function assay method was adopted from previously published papers testing the sodium/calcium exchange activity of NCX1 (Reeves and Sutko 1979; Reeves and Sutko 1983). Briefly, one tube of aliquoted membrane vesicle preparation was quickly thawed at 37°C. The same volume of pre-incubation buffer (20mM MOPS/Tris pH7.2, 160mM NaCl) was mixed with the thawed membrane vesicle preparation and incubated at 37°C for 20 minutes. Then the Na^+-loaded membrane vesicle preparation was added to 1ml of uptake buffer, which contained 160mM NaCl or KCl or LiCl, 25mM MOPS/Tris pH7.0, 100μM $CaCl_2$, and 2μCi/ml $^{45}CaCl_2$, at room temperature to initiate the uptake procedure. At certain time points, 150μl aliquots were taken out from the uptake mixture and immediately added into 3ml of ice cold quench buffer (150mM KCl and 1mM $LaCl_3$) to stop the reaction. These vesicles were then filtered through nitrocellulose filter paper (Millipore, pore size 0.3μm) using a 12-well filtering manifold (Millipore) and washed

twice using 5ml of ice cold quench buffer. For background radiation subtraction, 150µl of uptake buffer alone was added to 3ml ice cold quench buffer and filtered immediately. The filters were washed twice with 5ml of ice cold quench buffer. Finally the filters were collected into scintillation vials and counted in a liquid scintillation counter. These counts were analyzed and summarized using Microsoft Excel.

Other Ca^{2+} uptake conditions, such as lowered glucose concentration inside vesicles, lowered pH inside vesicles, altered Na^{+} and K^{+} concentrations, were also tried with similar procedures as described above.

2.2.11.2 Ca^{2+} imaging

MNT1 or B16 cells cultured on poly-D lysine coated coverslips were loaded with the Ca^{2+} sensitive dye Fura-2 by incubating the coverslip in 1ml of 5µM Fura-2 and 0.01% Pluronic F-127 (50µg Fura-2 diluted in 4µl of 20% Pluronic F-127, 6µl of DMSO, and 10ml of DMEM/25mM HEPES-TMA, pH7.4) for 40 minutes at room temperature. The Fura-2 loaded coverslip was then mounted in a perfusion chamber on the microscope stage.

To test whether there is surface NCKX expression in these two melanoma cell lines, the following perfusion procedure was used. The cells were first perfused with Na0K solution (145mM NaCl, 0.1mM $CaCl_2$, 1mM D-glucose, and 1mM HEPES-TMA, pH7.4) for 2 minutes at room temperature, and then the perfusion solution was switched to Li5K (140mM LiCl, 5mM KCl, 0.1mM $CaCl_2$, 1mM D-glucose, and 1mM HEPES-TMA, pH7.4). This perfusion protocol was used twice on each coverslip. Finally 100µl of 0.1M

ATP was added directly to the coverslip to stimulate the cells. Images were taken every 10 seconds.

To inhibit the V-type ATPase and test the working model for NCKX5 proposed by Cheng's group, the following perfusion procedure was used. Briefly, the cells were first perfused with Na5K solution (140mM NaCl, 5mM KCl, 0.1mM $CaCl_2$, 1mM D-glucose, and 1mM HEPES-TMA, pH7.4) for 2 minutes and then perfused with Na5K plus 1nM baflomycin for 2 minutes. Finally, 100µl of 0.1M ATP was added directly to the coverslip to stimulate the cells. Images were taken every second.

CHAPTER THREE

RESULTS

3.1 Amplification and subcloning of mouse NCKX5

Reverse transcription coupled polymerase chain reaction (RT-PCR) amplification was used to obtain the mouse NCKX5 clone. Mouse brain, kidney and B16 cell total RNA were used as the templates. The same amount of H_2O was used to substitute the total RNA templates, the reverse transcriptase, or the first strand cDNA, as negative controls for reverse transcription or PCR. The RT-PCR products were then analyzed on 1% agarose or 5% polyacrylamide gels. The results of the gel separation of RT-PCR products are shown in Figure 5 with panel A showing RT-PCR from mouse brain and kidney total RNA and panel B showing RT-PCR from B16 cell total RNA, both with negative controls. A single specific band of the same size, about 1.6kb, can be seen in each of the three lanes in which mouse brain, kidney, and B16 total RNA were used as templates. However, no bands can be seen in any of the negative control lanes, in which H_2O was used in substitution of the RNA template, the reverse transcriptase, or the first strand DNA. The size of the band is very similar to the length of the coding region of the reported mouse NCKX5 cDNA sequence in the database (Figure 6), which is also about 1.6kb. The 1.6kb band from B16 cell RNA was cut out and the DNA was eluted and sequenced directly using 3 primers: Ms-NK5-3, Ms-NK5-4, and Ms-NK5-R (Figure 6 and Table 2). The 1.6kb band from mouse brain and kidney RNA was cut out and the DNA was eluted. The eluted samples were digested with EcoRI and subcloned into the

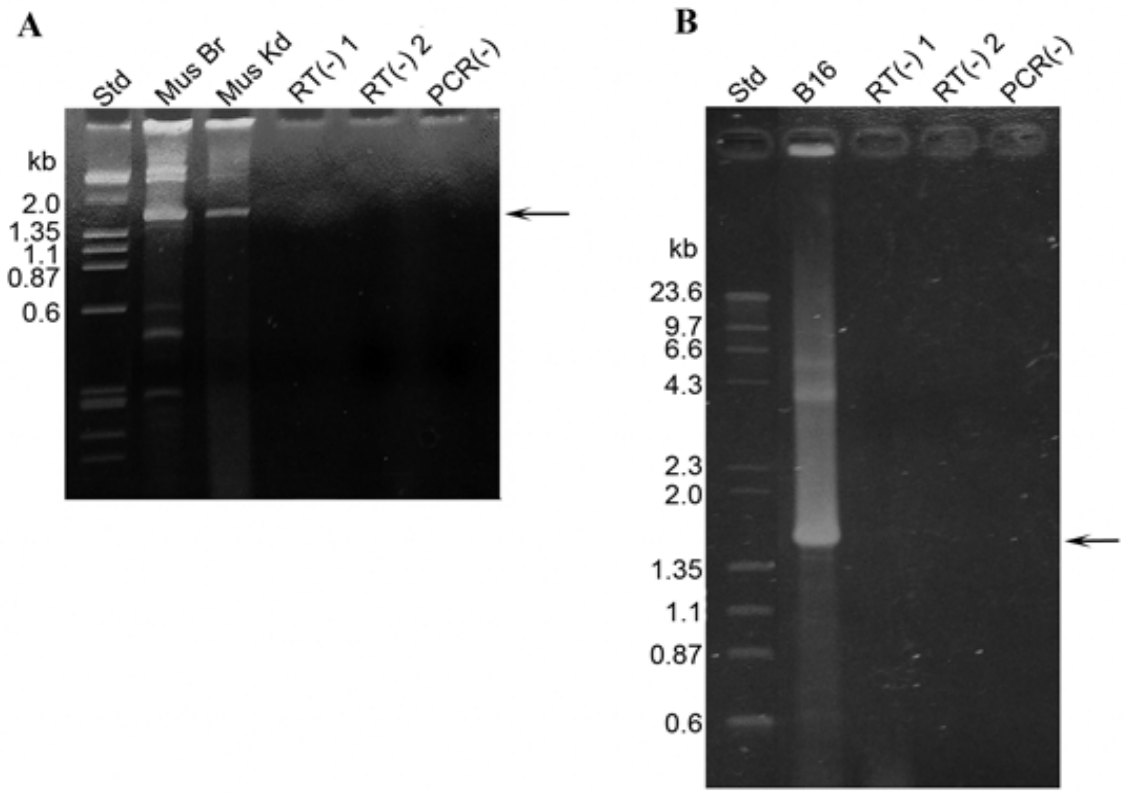

Figure 5. Results of RT-PCR. Five μg of mouse brain, kidney, and B16 cell total RNA was reverse transcribed and amplified using primer pair Mus NK5-F and Mus NK5-R (see Figure 5 and Table 2). **A** is a 5% polyacrylamide gel; **B** is a 1% agarose gel. Std: DNA standard; Br: total RNA from mouse brain; Kd: total RNA from mouse kidney; B16: total RNA from B16 cells; RT(-)1: negative control for reverse transcription, H_2O was used instead of reverse transcriptase, mouse brain total RNA (panel A) or B16 total RNA (panel B) were used as templates; RT(-)2: negative control for reverse transcription, H_2O was used instead of total RNA; PCR(-): negative control for PCR, H_2O was used instead of first strand DNA. For panel **A**, similar results were obtained from more than five independent experiments. For panel **B**, similar results were obtained from two independent experiments.

Figure 6. Mouse NCKX5 DNA sequence. Sequencing results of RT-PCR products from B16, mouse brain and kidney total RNA were identical with the sequence in the EST database. Primers used in this project for amplification of the whole mouse sequence, epitope insertion and amplification of DNA probes for Northern blotting are shown.

EcoRI site of pBlueScriptII SK (-).The clones were sequenced using T7 and T3 primers. The sequencing results showed that all three DNA sequences were identical with the mouse NCKX5 cDNA sequence (Figure 6) reported in the database.

3.2 Tissue distribution of NCKX5 transcripts

Total RNA samples isolated from a variety of mouse tissues and B16 cells were tested. Two digoxigenin-labeled DNA probes, one from the cytoplasmic loop region (from nucleotide 535-1088, Figure 6) and the other from the 5'-end region (from nucleotide 42 to 247, Figure 6) of mouse NCKX5 clone, were used. The results of the Northern blot analysis are shown in Figure 7 and Figure 8.

Figure 7 displays the Northern blotting result of various mouse tissues and B16 cell RNA using the probe from the cytoplasmic loop. Four major transcripts are visible in the blot. The smallest transcript is about 1.6kb and the next largest is about 2.0kb. These transcripts are strictly expressed in B16 cells, mouse eye and skin, with the most abundant expression observed in B16 cells and in mouse eye, and lower expression in mouse skin. A large transcript of about 10.5kb is mainly expressed in mouse eye and thymus, with lower expression in all other tissues tested. The largest transcript is around 11.0kb and mainly expressed in mouse brain and at lower levels in eye and thymus with a much lower level of expression in all other tissues tested.

A Northern blot comparing two different probes from the cytoplasmic region and 5'-end region of the mouse NCKX5 clone was also performed. The reason for doing this was to test if the N-terminus of the NCKX5 clone obtained from mouse brain and kidney, which express only the larger transcripts, was also present in the smaller transcripts found

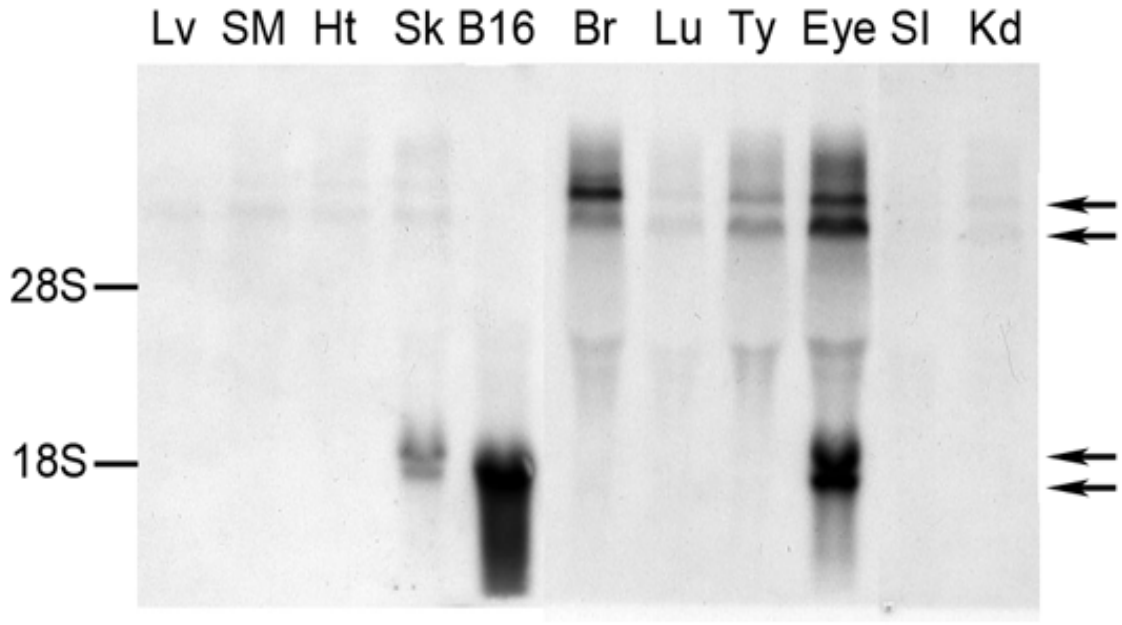

Figure 7. Tissue distribution of mouse NCKX5 transcripts. Ten μg of total RNA from each of the indicated mouse tissues or cell line was analyzed by Northern blot at high stringency using a digoxingenin-labeled DNA probe covering the entire cytoplasmic loop region of mouse NCKX5. Arrows indicate transcripts of different sizes. Lv: liver; SM: skeletal muscle; Ht: heart; Sk: skin; B16: B16 cell line; Br: brain; Lu: lung; Ty: thymus; SI: small intestine; Kd: kidney. Similar results were observed from two independent experiments. Figure courtesy of Xiao-Fang Li.

in mouse eye, skin and B16 cells. Total RNA from B16 cell line, mouse eye and skin were used in this experiment. The result of this comparison is shown in Figure 8. In panel A, the RNA samples were hybridized with the probe covering the whole cytoplasmic loop region (this figure was generated by cutting and combining the corresponding lanes in Figure 7 without other adjustments) and in panel B, the RNA samples were hybridized with the probe covering the entire 5'-end region. The expression patterns are very similar between these two panels. Two major transcripts, both of which are doublets, can be seen, one 1.8kb and the other 10.5kb. The relative intensity of the large to the small NCKX5 bands seen in the eye lane appears similar between panel A and B. Also the relative expression level of the smaller transcripts is retained between panel A and B, with B16 > eye > skin. This result suggests that the 5'-end found in the NCKX5 clone is also present in the major 1.8kb transcripts.

It is notable that two transcripts of different sizes were detected in the experiments. B16 cells express only the 1.8kb transcript whereas mouse brain expresses only the 10.5kb transcript. Since the sequence of the RT-PCR products from B16 cell RNA and mouse brain RNA was identical, and the Northern blotting results with the two different probes were also identical, these data suggest that the coding region of 5'-ends of long and short transcripts are likely to be the same. It is likely that both the short and long transcripts encode the same protein, but have different extents of untranslated region at either 3'-end or 5'-end.

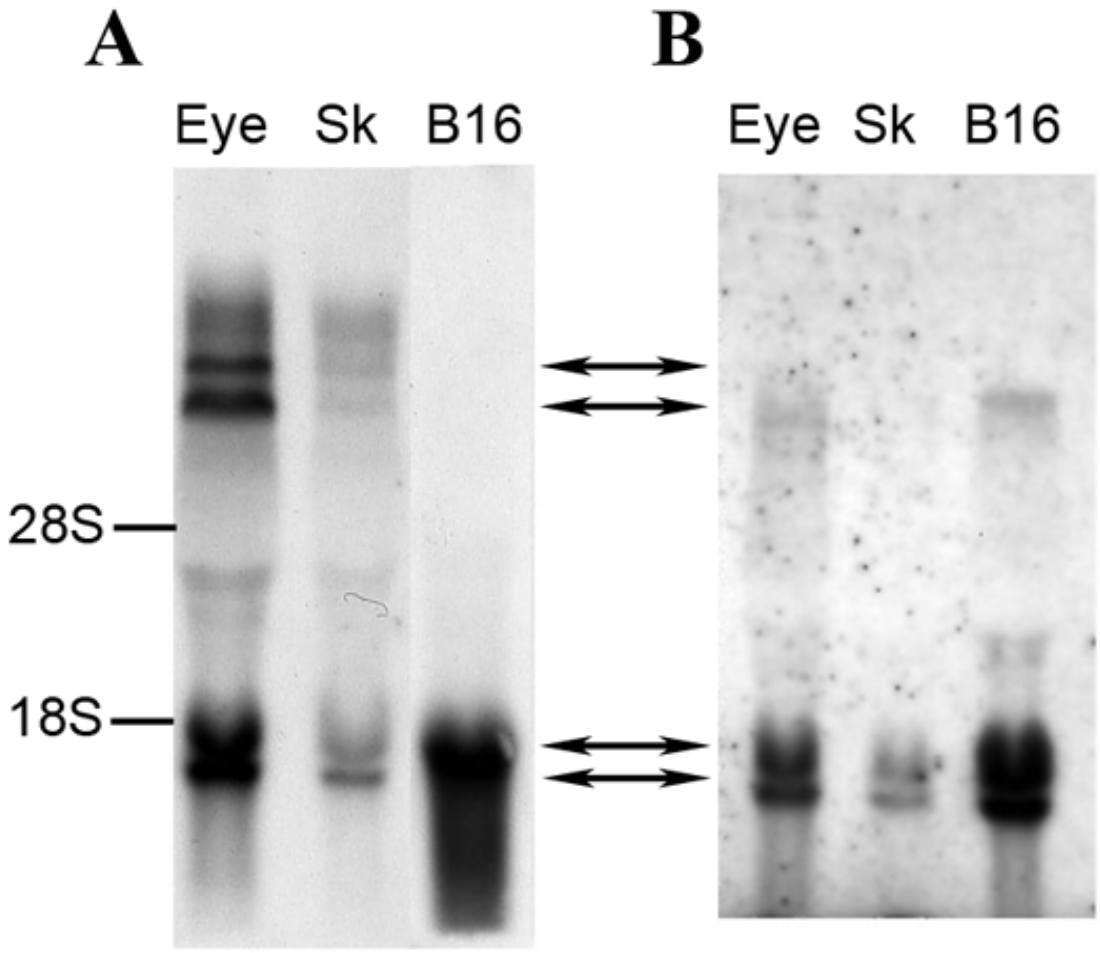

Figure 8. Northern blot results comparing two probes. Ten μg of total RNA from each of the indicated mouse tissues or cell line was analyzed by Northern blot at high stringency using a digoxigenin-labeled DNA probe either covering the cytoplasmic loop region or covering the 5'-end region (Figure 6). **A** shows the result from the cytoplasmic loop probe; **B** shows the result from the 5'-end probe. Sk: skin; B16: B16 cell line. Figure courtesy of Xiao-Fang Li.

3.3 Detection of NCKX5 protein expression

3.3.1 Detection of recombinant NCKX5 protein expression in HEK293 cells

Microsome preparations made from HEK293 cells transfected with mouse full length wild type NCKX5 construct, FLAG or HA tagged NCKX5 constructs, or pcDNA3.1(+) alone were analyzed by immunoblot. Twenty micrograms of each microsomal preparation was separated on a 9% SDS-PAGE and transferred to a nitrocellulose membrane. The membrane was probed with either anti-NCKX5 serum or peptide pre-absorbed anti-NCKX5 serum as a negative control. The results of the immunoblot are shown in Figure 9. Panel A shows the membrane probed with anti-NCKX5 serum and panel B shows the membrane probed with peptide pre-absorbed anti-NCKX5 serum. In panel A, two major bands are visible from lanes in which various NCKX5 microsome samples were loaded. The larger one is about 52kDa and the smaller one is about 42kDa. However, in the pcDNA3.1(+) microsome loaded lane, no bands of similar size are visible. In panel B, no bands of the corresponding sizes, 52kDa and 42kDa, can be visualized in any of the lanes. The comparisons between NCKX5 microsome loaded lanes and vector microsome loaded lane and between anti-NCKX5 serum and peptide pre-absorbed serum probed membranes indicate that the bands detected in panel A are the recombinant NCKX5 protein expressed in transfected HEK293 cells. The 52kDa band is of similar size as predicted according to the length of mature mouse NCKX5 protein, but the 42kDa band is smaller than predicted.

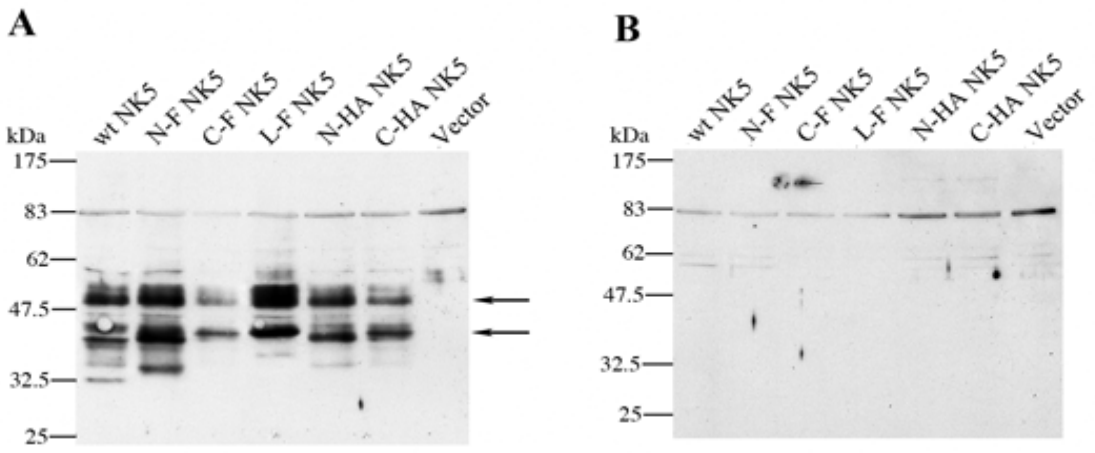

Figure 9. Detection of NCKX5 protein expression in extracts from transfected HEK293 cells. Twenty μg of protein from transfected HEK293 cell microsome preparations was analyzed by immunoblot. **A** shows membrane probed with anti-NCKX5 serum; **B** shows membrane probed with peptide pre-absorbed anti-NCKX5 serum. Protein size markers are labeled at the left of each panel. wt NK5: wild type NCKX5; N-F NK5: NCKX5 FLAG tagged at the N-terminus; C-F NK5: NCKX5 FLAG tagged at the C-terminus; L-F NK5: NCKX5 FLAG tagged in the cytoplasmic loop; N-HA NK5: NCKX5 HA tagged at the N-terminus; C-HA NK5: NCKX5 HA tagged at the C-terminus; vector: pcDNA3.1(+). Similar results were obtained from over five independent experiments.

3.3.2 Detection of endogenous NCKX5 protein in melanoma cell lines

It has been reported that NCKX5 expression is highest in pigmented cells, like skin melanocytes (Lamason, Mohideen et al. 2005; Chi, Valencia et al. 2006), and the Northern blot results also display a high expression level of the 1.6kb NCKX5 transcript in mouse melanoma cell line B16. Thus two melanoma cell lines of different origins, B16 from mouse and MNT1 from human, were chosen to test endogenous NCKX5 protein expression. Twenty micrograms protein of post nuclear preparation from B16 and MNT1 cells were separated on 9% SDS-PAGE and analyzed by immunoblot together with 20μg each of microsomal preparation from HEK293 cells transfected with either wild type NCKX5 or pcDNA3.1(+) as a positive and a negative control respectively. The immunoblot results are shown in Figure 10. In panel A, the membrane was probed with anti-NCKX5 serum. The bands in the positive control lane, wt NK5, are the same size as seen in Figure 9. In the lane where B16 post nuclear preparation was loaded, a 42kDa band, which is less intense than the corresponding band in wt NK5 lane, can be seen. In the lane where MNT1 post nuclear preparation was loaded, an even fainter band at 42kDa and another band around 48kDa are visible. But none of the above bands can be seen in pcDNA3.1(+) lane. In panel B, the membrane was probed with peptide pre-absorbed anti-NCKX5 serum. The aforementioned bands in panel A are no longer visible, whereas the non-specific bands at 60kDa and larger in the cell line extracts are almost the same in both panels of Figure 10. This suggests the 48kDa and 42kDa bands in B16 and MNT1 lanes in panel A correspond to the expression of endogenous NCKX5 protein.

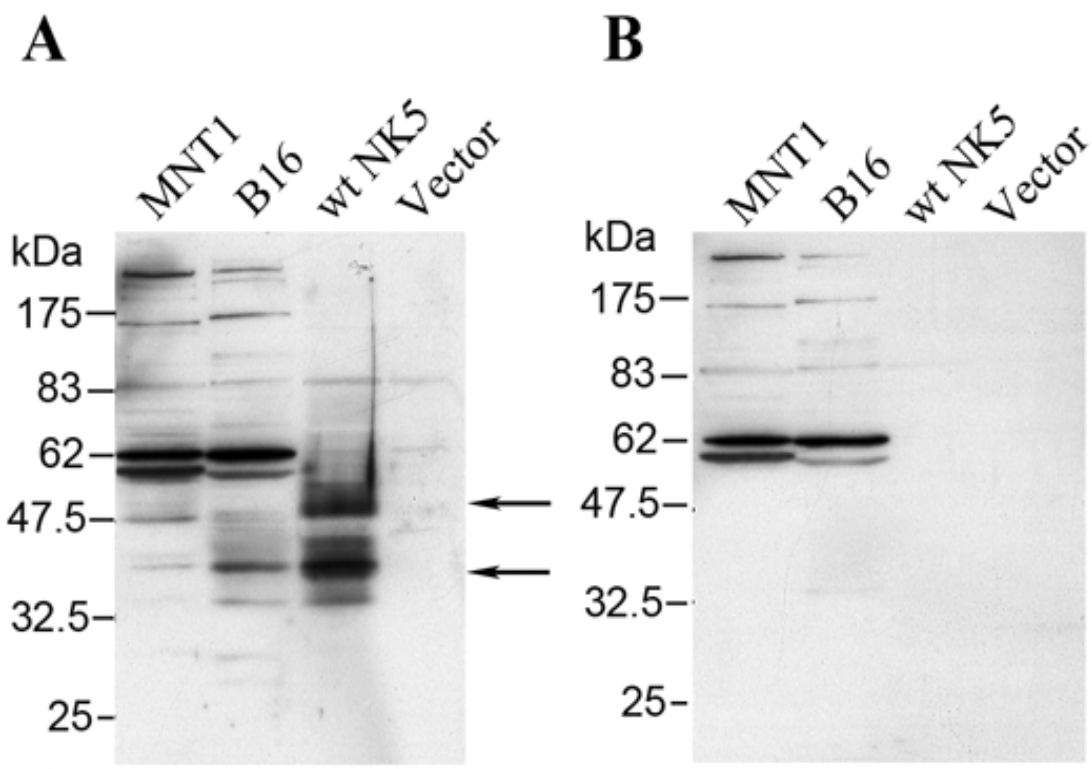

Figure 10. Detection of endogenous NCKX5 protein expression in melanoma cell lines, B16 and MNT1. Twenty μg of protein from post nuclear extracts of B16 and from MNT1 cells and microsome preparations of transfected HEK293 cells was analyzed by immunoblot. **A** shows membrane probed with anti-NCKX5 serum; **B** shows membrane probed with peptide pre-absorbed antiserum. Protein size markers are labeled at the left of each panel. MNT1: post nuclear extracts from MNT1 cells; B16: post nuclear extracts from B16 cells; wt NK5: microsome preparations from wild type NCKX5 transfected HEK293 cells; vector: microsome preparations from pcDNA3.1(+) transfected HEK293 cells. Similar results were obtained from four independent experiments.

In contrast to the detection of NCKX5 expressed in HEK293 cells, the specific NCKX5 proteins in melanoma cell extracts detected with anti-NCKX5 serum were relatively weak, and several prominent non-specific bands were detected. Therefore, affinity purified NCKX5 antibody was tested against these samples. The results of the immmunoblot comparing purified antibody and anti-serum are shown in Figure 11. In panel A, the membrane was probed with anti-NCKX5 serum and in panel B the membrane was probed with purified anti-NCKX5 antibody. In both panels, bands of size 52kDa and 42kDa are visible in wild type NCKX5, B16, and MNT1 lanes but not in pcDNA3.1(+) lane. Although the signal from the affinity purified NCKX5 antibody was weaker than that from the anti-NCKX5 serum, it is obvious that the purified antibody generated a clearer result and the non-specific bands appearing in the serum probed membrane were diminished in the purified antibody probed membrane. The same amount, 20μg, of membrane protein was loaded in each lane, but the band in MNT1 lane is obviously weaker than the one in B16 lane. This might be because the MNT1 cells are of human origin but the antibody was raised against mouse NCKX5 sequence. There are three amino acids difference in the antigen regions between mouse NCKX5 protein and human NCKX5 protein. Therefore, the antibody may bind more weakly to human NCKX5 protein than it does to the mouse one. It is also possible that there is different amount of NCKX5 protein present in the microsome preparations and post nuclear extracts from the two cell lines.

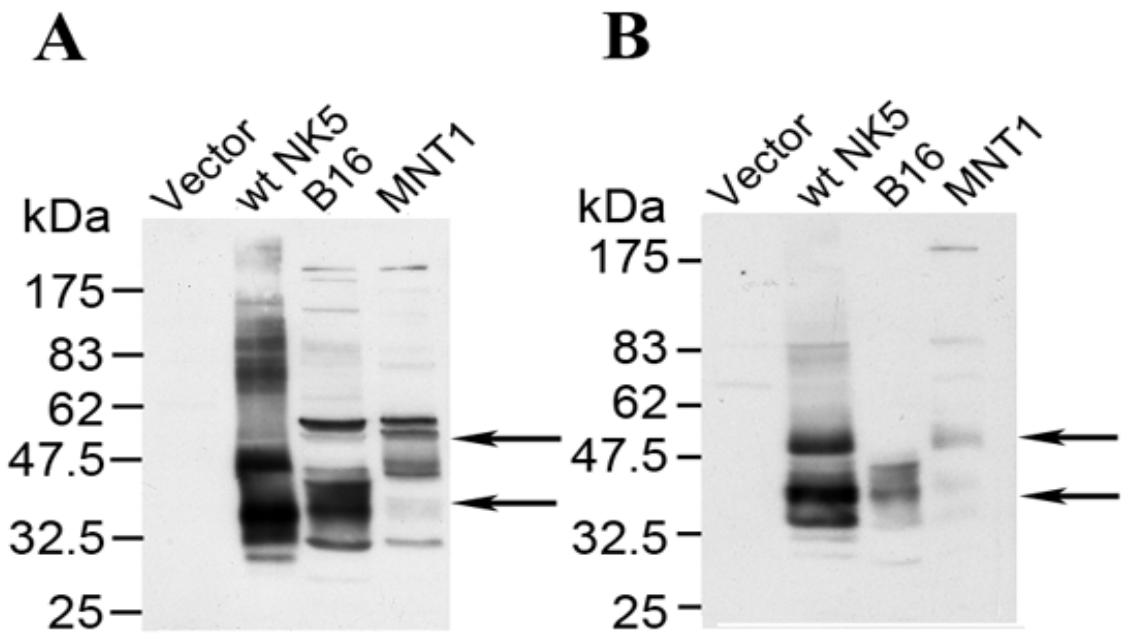

Figure 11. Detection of NCKX5 protein expression in melanoma cell lines using affinity purified antibody. Twenty micrograms of protein from microsomal preparations of B16, MNT1 cells and wild type NCKX5 or pcDNA3.1(+) transfected HEK293 cells was analyzed by immunoblot. **A** shows membrane probed with anti-NCKX5 serum; **B** shows membrane probed with affinity purified antibody. Protein size markers are labeled at the left of each panel. MNT1: microsomal preparation from MNT1 cells; B16: microsomal preparation from B16 cells; wt NK5: microsomal preparation from wild type NCKX5 transfected HEK293 cells; vector: microsomal preparation from pcDNA3.1(+) transfected HEK293 cells. Similar results were obtained from three independent experiments. Figure courtesy of Yiqian Wang.

3.4 N-glycosidase F digestion of NCKX5 protein

It is noticeable that two bands were detected by immunoblot. My hypothesis about this observation is that these two bands are due to different levels of glycosylation on the same NCKX5 protein. To test this hypothesis, N-glycosidase F digestion was performed. 20μg each of wild type NCKX5 and three forms of FLAG epitope tagged NCKX5 microsomes were digested by N-glycosidase F for two hours at 37°C. In control samples the same amount of H_2O was used in substitution of N-Glycosidase F. pcDNA3.1(+) microsome was included as a negative control for the immunoblot as well. The result is shown in Figure 12. In the lanes where samples were not digested by N-glycosidase F, two major bands are visible and both of them are of the same sizes as the bands seen in the immunoblot experiments described above. In the lanes where samples were digested by N-glycosidase F, the two bands merged together into one major band of even smaller size, about 37kDa. This suggests that the two bands appearing in the non-digested lanes are two forms of N-glycosylated NCKX5 protein with different glycosylation levels at the same N-glycosylation site. It is worthwhile noting that in N-glycosidase F digested lanes, the size of the FLAG tagged NCKX5 bands is a little bigger than that of the wild type NCKX5 band. This suggests the inserted epitope was present in the protein. It is also notable that there are still two bands, in the N-F NK5 lane even after N-glycosidase F digestion. Since the position where FLAG epitope was inserted is very close to the predicted peptide cleavage site, it is possible that the inserted epitope interferes with the efficiency of signal peptidase cleavage.

The N-glycosidase F digestion experiment was also performed on B16 and MNT1

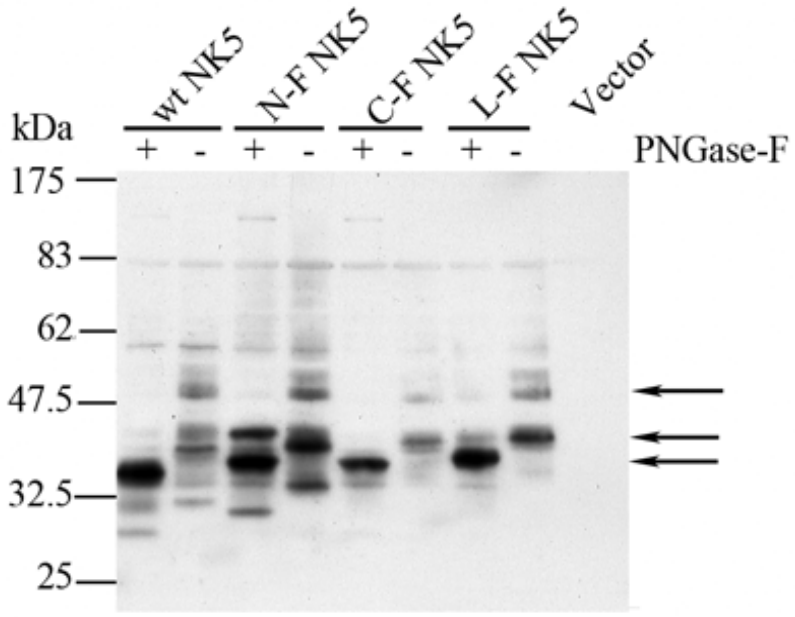

Figure 12. N-glycosidase F digestion of NCKX5 microsome preparations from tranfected HEK293 cells. Twenty μg of protein from NCKX5 microsome preparations, either digested with PNGase-F (+) or treated without enzyme (-), was analyzed by immunoblot using anti-NCKX5 serum. wt NK5: wild type NCKX5; N-F NK5: NCKX5 FLAG tagged at the N-terminus; C-F NK5: NCKX5 FLAG tagged at the C-terminus; L-F NK5: NCKX5 FLAG tagged at the cytoplasmic loop; vector: pcDNA3.1(+). Similar results were obtained from two independent experiments.

post nuclear preparations. Wild type NCKX5 was included as a positive control and the same amount of H_2O was used in substitution of N-glycosidase F as a negative control. The result is shown in Figure 13. In panel A, the membrane was probed with anti-NCKX5 serum. After N-glycosidase F digestion, the two bands, 52kDa and 42kDa, in B16 and MNT1 lanes merged into one major smaller band, about 37kDa, that migrated at the same size as the wild type NCKX5 band in HEK293 cell microsomes. In panel B, the membrane was probed with peptide pre-absorbed anti-NCKX5 serum, demonstrating the specific nature of the 52, 42, and 37kDa bands. In Figures 10, 11 and 13, it is also noticeable that the NCKX5 protein in B16 cells and MNT1 cells are of different levels of N-glycosylation. It seems MNT1 cells mostly express NCKX5 protein of size 52kDa whereas B16 cells mostly express NCKX5 protein of size 42kDa, but both proteins migrate at 37kDa following PNGase-F treatment.

3.6 Subcellular localization of NCKX5 protein

3.6.1 Localization of recombinant NCKX5 protein in transfected HEK293 cells

HEK293 cells transfected with the wild type mouse NCKX5 construct or with pcDNA3.1(+) alone, either permeablized with Triton X-100 or left unpermeablized, were stained using either anti-NCKX5 serum or peptide pre-absorbed anti-NCKX5 serum. The staining results are shown in Figure 14. Panel A shows the permeablized, anti-NCKX5 serum stained HEK293 cells transfected with wild type NCKX5. Cells expressing NCKX5 protein show a specific staining pattern while those cells without NCKX5 protein expression only show similar staining signal level as seen in untransfected cells. Generally speaking, about 30%-40% of the cells were transfected and expressing the

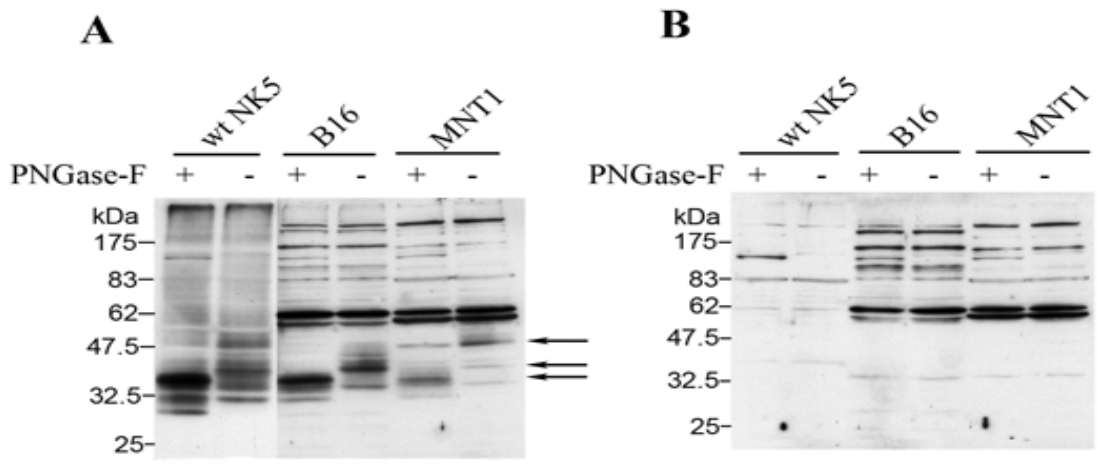

Figure 13. N-glycosidase F digestion of post nuclear extracts from melanoma cell lines. Twenty μg of protein from post nuclear extracts of B16 or MNT1 cells and microsome preparation from wild type NCKX5 transfected HEK293 cells, either digested with PNGase-F (+) or treated without enzyme (-), was analyzed by immunoblot. NCKX5 microsome preparation was included as a positive control. A shows membrane probed with anti-NCKX5 serum; **B** shows membrane probed with peptide pre-absorbed antiserum. Note: the two wild type NCKX5 lanes in panel A were cut from a shorter exposure film from the same experiment in order to achieve similar intensity of the bands of interest. Similar results were obtained from three independent experiments.

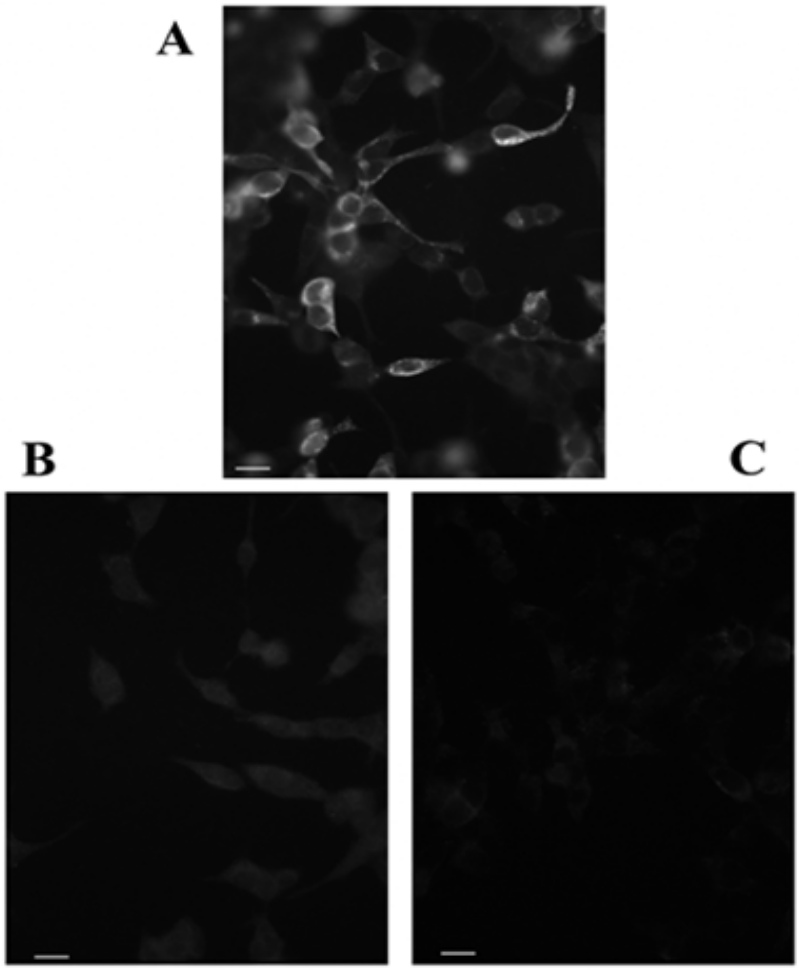

Figure 14. Subcellular localization of NCKX5 protein in transfected HEK293 cells. Immunostaining was performed on transfected HEK293 cells, either permeablized with 0.1% Triton X100 or left unpermeablized using anti-NCKX5 serum. **A** shows wild type NCKX5 transfected HEK293 cells, permeablized; **B** shows pcDNA3.1(+) transfected HEK293 cells, permeablized; **C** shows wild type NCKX5 transfected HEK293 cells, unpermeablized. Primary antibody: anti-NCKX5 serum; secondary antibody: Cy3 conjugate anti-rabbit antibody. All panels were photographed in parallel using the same exposure settings. Scale bar indicates 50μm. Similar results were obtained from three independent experiments.

recombinant NCKX5 protein. Panel B shows permeablized, anti-NCKX5 serum stained HEK293 cells transfected with pcDNA3.1(+) alone. HEK293 cells were treated exactly the same way as those cells in panel A except the DNA construct for transfection was pcDNA3.1(+). All cells show similar staining signal as the background. The comparison between panel A and B suggests that the staining in panel A is the recombinant NCKX5 protein expressed in HEK293 cells. In panel C, the HEK293 cells were transfected with wild type NCKX5 construct and stained using anti-NCKX5 serum. The only difference between these cells and the cells in panel A and B is these cells were not permeablized. The staining of the cells in panel C also exhibits only background staining signal.

The epitope for the NCKX5 antibody resides in the glycosylated loop, which would be exposed to the cell exterior if NCKX5 were trafficked to the cell surface plasma membrane. The lack of staining in non-permeablized HEK293 cells in panel C strongly suggests that the recombinant NCKX5 protein was located inside the cells, unlike other NCKX family members, which are located on the plasma membrane of the cells.

Figure 15 shows permeablized HEK293 cells expressing wild type NCKX5 protein stained by anti-NCKX5 serum at higher magnification. It is notable that the NCKX5 staining shows a pattern suggestive of association with intracellular organelles. Most of NCKX5 staining was concentrated close to the nucleus and present as a punctate pattern through out the cytoplasm

3.6.2 Localization of endogenous NCKX5 protein in B16 cells

B16 cells were fixed and permeablized using a mixture of ice cold 70% methanol and 30% acetone. These treated cells were stained with either purified anti-NCKX5

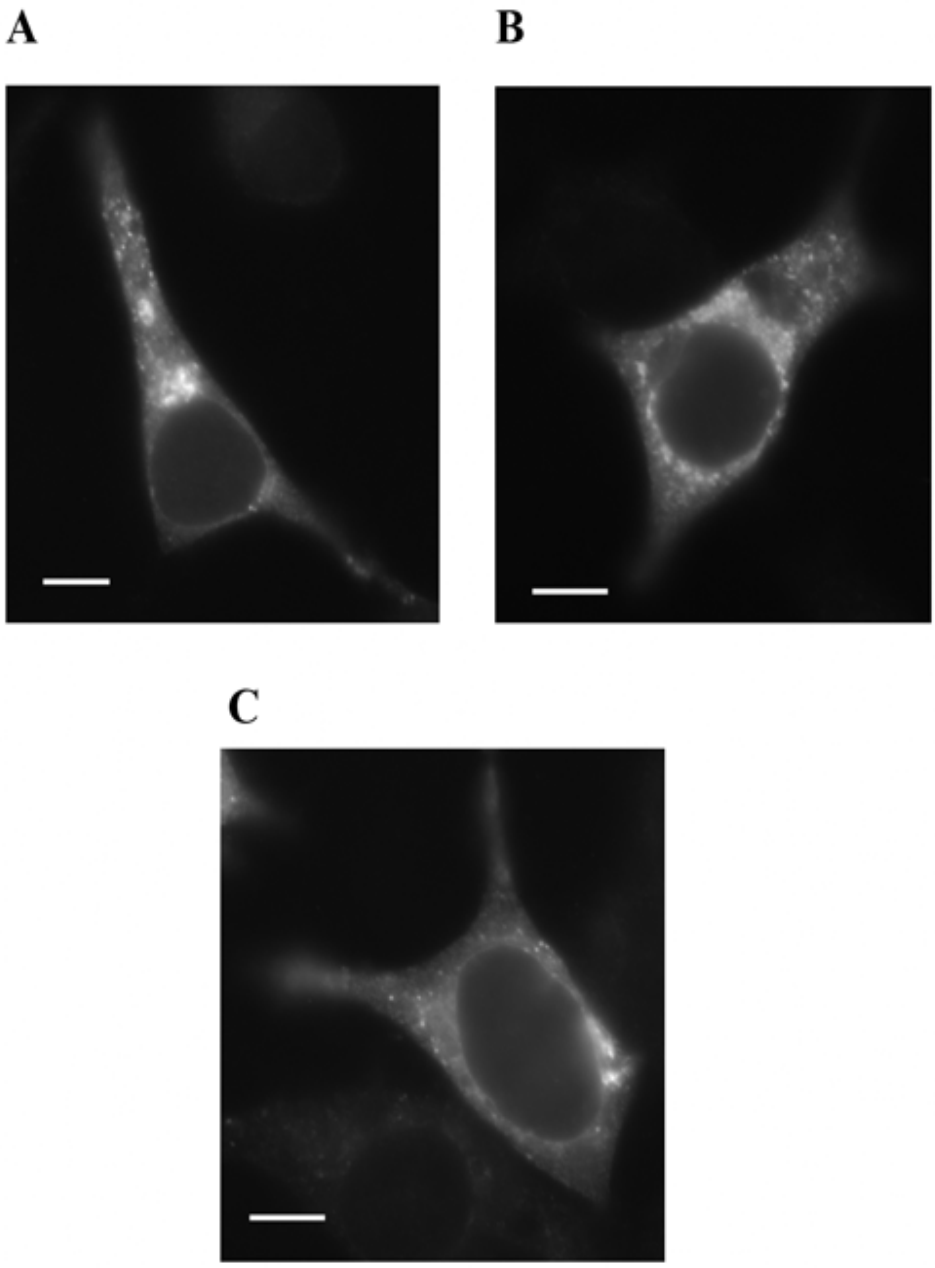

Figure 15. Subcellular localization of NCKX5 protein in transfected HEK293 cells. Examples from three cells are shown. All three cells were permeablized, stained with anti-NCKX5 serum, and observed under higher magnification. Scale bar indicates 10μm.

antibody or peptide pre-absorbed purified anti-NCKX5 antibody. The staining results are shown in Figure 16. As expected, it can be seen that in panel A, almost every cell stained for NCKX5, even though the signal is not as strong as that in NCKX5 transfected HEK293 cells. In panel B, the cells were stained with peptide pre-absorbed purified antibody. All cells show a similar level of staining no different than background. Panel C and D show examples from two B16 cells stained with purified antibody. The staining pattern for NCKX5 in B16 cells is very similar to that observed for wild type NCKX5 expressed in HEK293 cells. Staining is localized predominantly to one side of the perinuclear region and as a punctate pattern within the cytoplasm.

3.7 Function study of NCKX5 protein – Ca^{2+} uptake into membrane vesicles

My data and those of others (Lamason, Mohideen et al. 2005; Chi, Valencia et al. 2006) demonstrated that the NCKX5 protein was located inside the cells. Therefore, it was not feasible to test NCKX5 function on intact cells using a standard Ca^{2+} imaging method with perfusion switches as has been employed previously for the surface expressed NCKX family members (Tsoi, Rhee et al. 1998; Kraev, Quednau et al. 2001; Li, Kraev et al. 2002). Instead, a Ca^{2+} uptake assay was developed based on assays previously developed for NCX1 (Reeves and Sutko 1979; Reeves and Sutko 1983).

Membrane vesicles were prepared separately from wild type NCKX5, NCX1, NCKX2, and pcDNA3.1(+) transfected HEK293 cells, MNT1 and B16 cells. All the membrane preparations used in uptake assays were tested by immunoblot to ensure proper expression of the proteins of interest prior to the uptake procedure. All vesicles were loaded with Na^+ prior to the initiation of uptake by pre-incubation with high Na^+

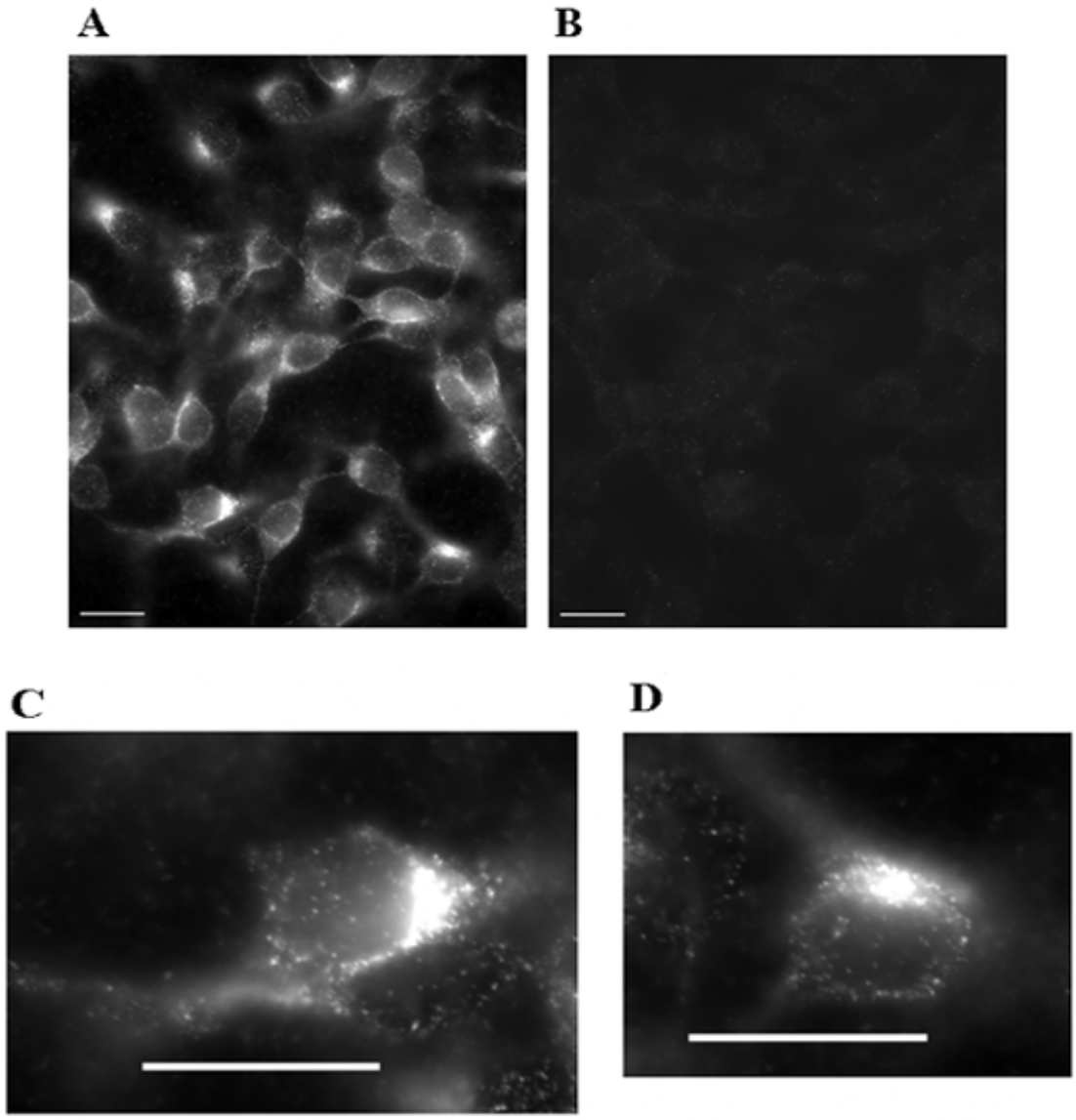

Figure 16. Subcellular localization of endogenous NCKX5 protein in B16 cells. B16 cells were permeablized and stained. **A** shows B16 cells stained with affinity purified antibody; **B** shows B16 cells stained with peptide pre-absorbed antibody. **C** and **D** are examples of two cells from panel A. Panel **A** and **B** were photographed in parallel using the same exposure settings. Scale bar indicates 20μm. Figure courtesy of Yiqian Wang. Similar results were obtained from five independent experiments.

solution at 37ºC. Then the Na^+-loaded vesicles were diluted into Na^+- or K^+- or Li^+-containing uptake buffer. At certain time points, aliquots were taken out, quenched and filtered. The results of Ca^{2+} uptake are shown in Figures 17 and 18.

Figure 17 demonstrates the uptake activities of NCX1 (circles), NCKX2 (squares), NCKX5 (triangles), and pcDNA3.1(+) (diamonds) microsomes diluted into K^+-containing (filled symbols), or Na^+-containing (open symbols) uptake buffers respectively. In the presence of an inside to outside Na^+ gradient, i.e. when diluted into K^+ uptake buffer, NCX1 and NCKX2 containing vesicles displayed a time-dependent Ca^{2+} uptake that saturated within one minute. No comparable uptake activity was observed in vector transfected cells or vesicles diluted into Na^+ buffer that experienced no Na^+ gradient. Vesicles from cells transfected with NCKX5 displayed no uptake activity greater than the negative controls in this system. These observations suggest that the recombinant NCKX5 protein expressed in HEK293 cells may be not functional.

Figure 18 shows the results of Ca^{2+} uptake from B16 (open symbols) and MNT1 (closed symbols) microsome preparations. When diluted into K^+ uptake buffer (squares), both B16 and MNT1 microsomes also showed a strong time-dependent Ca^{2+} uptake activity very similar to that observed in membranes from NCX1 and NCKX2 transfected HEK293 cells. Compared to the significant increase in Ca^{2+} uptake observed above, these microsomes only showed slight increases when diluted into Na^+ uptake buffer (triangles) or Li^+ uptake buffer (circles). These observations demonstrate that the uptake activity depends on Na^+ concentration gradient and the presence of K^+, which is typical of NCKX members.

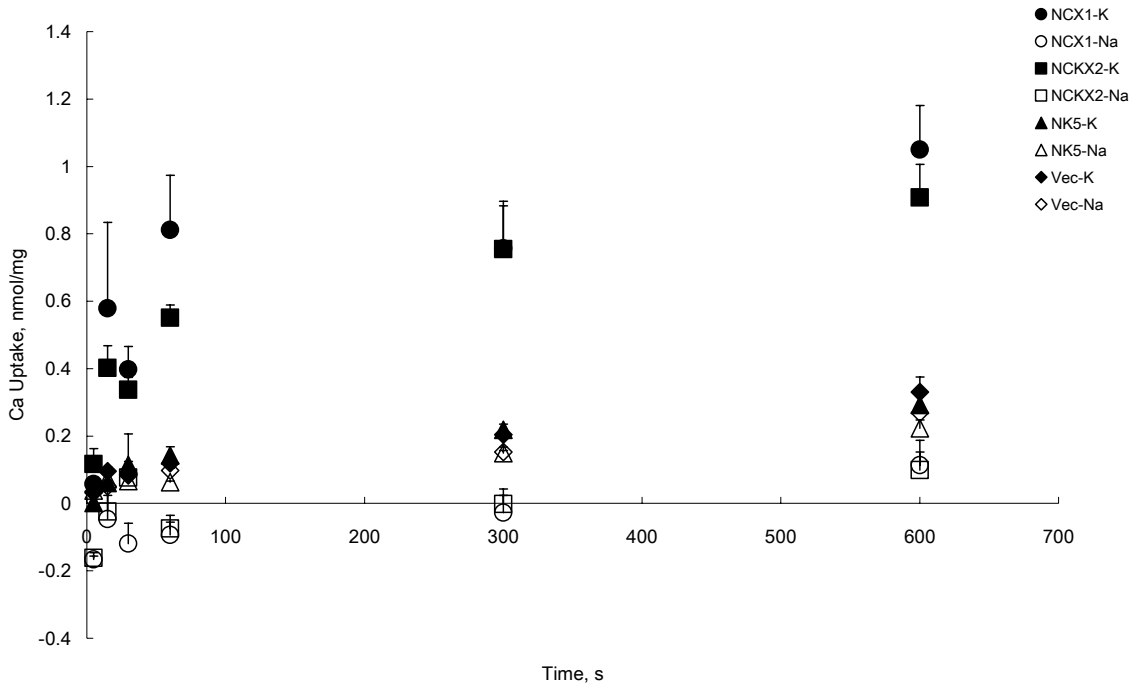

Figure 17. Ca^{2+} uptake into membrane vesicles from transfected HEK293 cells. Circles represent NCX1 containing membrane vesicles. Squares represent NCKX2 containing vesicles. Triangles represent NCKX5 containing vesicles. Diamonds represent vesicles from pcDNA3.1(+) transfected HEK293 cells. Closed symbols indicate membrane vesicles were diluted into K^+ uptake buffer. Opened symbols indicate membrane vesicles were diluted into Na^+ uptake buffer. Time points at which aliquots were removed: 5s, 15s, 30s, 60s, 300s, and 600s. Each data point is calculated from three parallel samples. Background counts have been subtracted. Error bars show the standard error associated with each data point. Similar results were obtained from at least three independent experiments using different batches of membrane preparations.

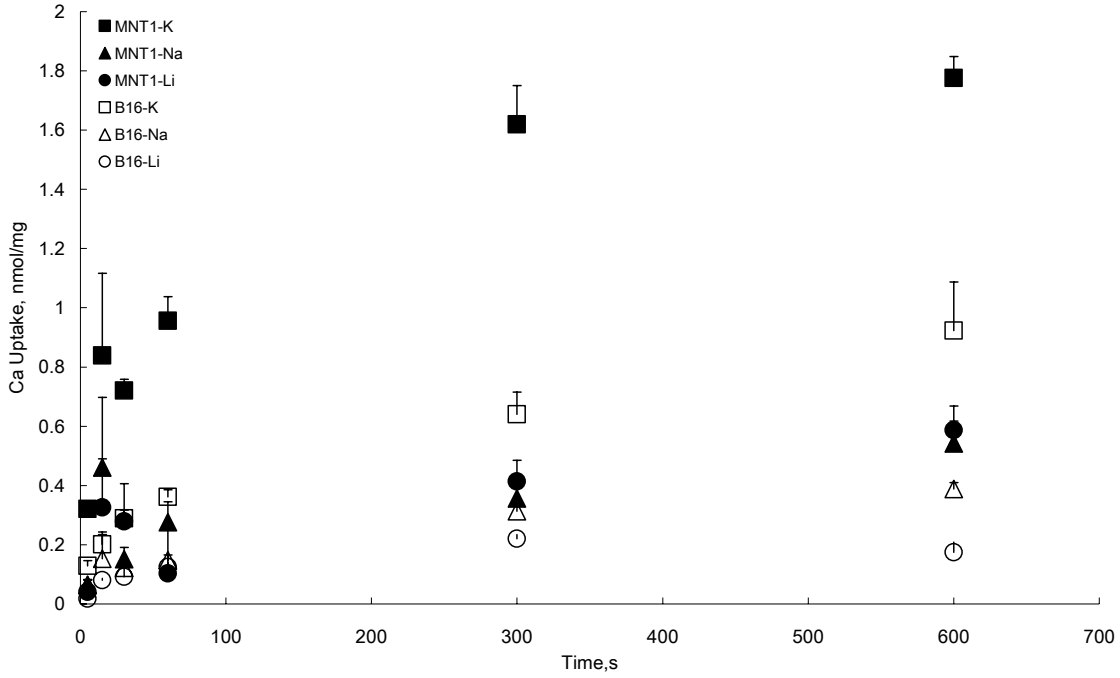

Figure 18. Ca^{2+} uptake into membrane vesicles from B16 and MNT1 cells. The closed symbols represent Na^+-loaded microsome preparations from MNT1 cells diluted into different uptake buffers and open symbols represent Na^+-loaded microsome preparations from B16 cells diluted into different uptake buffers. The squares represent membrane vesicles that were diluted into K^+ uptake buffer. The triangles represent membrane vesicles that were diluted into Na^+ uptake buffer. The circles represent membrane vesicles that were diluted into Li^+ uptake buffer. Time points at which aliquots were removed: 5s, 15s, 30s, 60s, 300s, and 600s. Each data point is calculated from three parallel samples. Background counts have been subtracted. Error bars show the standard error associated with each data point. Similar results were obtained from two independent experiments using two different batches of membrane preparations.

Figure 19 demonstrates the results of the detection of NCKX2, 3, 4, and 5 expression by RT-PCR and immunoblot in the two melanoma cell lines. Specific bands of expected size were observed for NCKX5 (383bp) and NCKX4 (761bp), and weakly for NCKX3 (509bp) in MNT1 cells. NCKX5 and NCKX4 expression were also detected in B16 RNA by PCR (panel B). There was no evidence for NCKX2 expression at either mRNA level in MNT1 cells (panel A) or protein level in B16 cells (panel B). As NCKX4 expression was detected in MNT1 and B16 cells, the Ca^{2+} uptake activity observed in the microsome preparations from MNT1 and B16 cells may not be due to only NCKX5. However, a considerable amount of experimental data from immunostaining and function studies showed other NCKX members (NCKX1-4) are all localized on the cell surface (Tsoi, Rhee et al. 1998; Kraev, Quednau et al. 2001; Li, Kraev et al. 2002; Schnetkamp 2004), therefore Ca^{2+} imaging was performed to investigate if surface NCKX activity could be detected in these two cell lines. When switching from Na^{+} containing solution to K^{+} and Li^{+} containing solution (Kraev, Quednau et al. 2001; Li, Kraev et al. 2002), no Fura-2 ratio changes were observed (data not shown). This result suggested that although low levels of NCKX4 and possibly NCKX3 transcripts were present, these may not be expressed as functional protein in MNT1 and B16 cells and, consequently, the uptake activity observed in these experiments likely corresponds to NCKX5 activity.

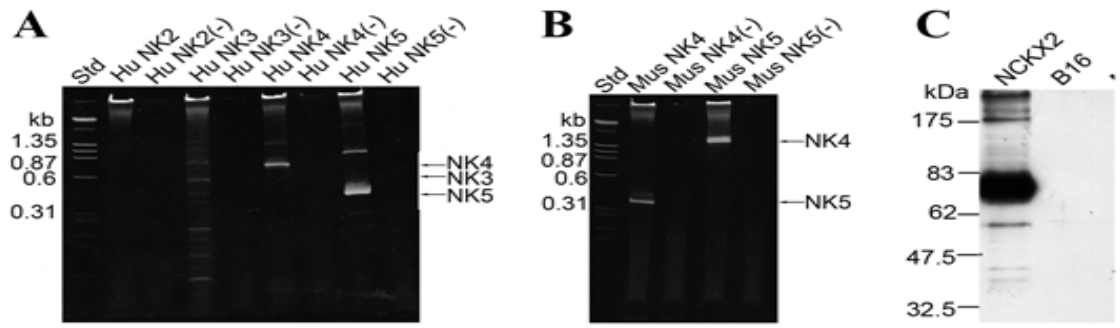

Figure 19. Detection of NCKX2, 3, 4, and 5 expression in MNT1 and B16 cells. A shows the RT-PCR products from MNT1 cell total RNA analyzed on a 5% acrylamide gel. **B** shows the RT-PCR products from B16 cell total RNA analyzed on a 5% acrylamide gel. Std: DNA standard; Hu NK2-5 indicates the RT-PCR products using human NCKX2-5 primer pair and MNT1 total RNA; Hu NK2-5 (-) indicates the RT-PCR products using human NCKX2-5 primer pair and H_2O; Mus NK4-5 indicates the RT-PCR products using mouse NCKX4-5 primer pair and B16 total RNA; Hu NK4-5 (-) indicates the RT-PCR products using human NCKX4-5 primer pair and H_2O. **C** shows the immunoblot result of microsome preparations from B16 cells and NCKX2 transfected HEK293 cells. The membrane was probed with F antibody (anti-NCKX2).

CHAPTER FOUR

CONCLUSION AND DISCUSSION

This study aimed to gain more knowledge about the biochemical and molecular properties of mammalian NCKX5. My results revealed that mouse NCKX5 has four major transcripts, 1.8kb, 2.0kb, 10.5kb, and 11kb and their relative expression level in various tissues. NCKX5 protein expression could be detected by immunoblot using anti-NCKX5 serum from transfected HEK293 cells and in B16 and MNT1 cells. Two major bands, 42kDa and 52kDa, which correspond to the same protein with different glycosylation levels, have been demonstrated. Immunofluoresence analysis showed NCKX5 was mainly localized on one side of perinuclear area in transfected HEK293 cells and in B16 cells, and distributed in a puctate pattern. Time-, Na^+ gradient-, and K^+-dependent, Ca^{2+} uptake activity was observed from membrane preparations of B16 and MNT1 cells but no comparable activity was observed from membrane preparations of transfected HEK293 cells.

4.1 Tissue distribution study

A previous study (Lamason, Mohideen et al. 2005) determined NCKX5 mRNA expression level in mouse tissues using the technique of quantitive real-time PCR. The results of the Northern blotting in our study confirmed the relative expression level of mouse NCKX5 mRNA in various mouse tissues and the melanoma cell line as reported in that study. Importantly, our data demonstrated the existence of four transcripts with the size of 11kb, 10.5kb, 2.0kb and 1.6 kb respectively (Figure 7). As the coding region of

mouse NCKX5 cDNA is only about 1.6kb, the 1.6kb transcript is adequate to cover the whole coding region. Because we were able to amplify NCKX5 with the identical sequence from mouse brain total RNA, which expresses predominantly the 11kb transcript form, and from B16 cell total RNA, which expresses only the two smaller transcripts, 1.6kb and 2.0kb, we conclude that both sets of transcripts encode the same protein. Because the 5'-end of the coding region seems to be the same by comparing the Northern blot result of probes from cytoplasmic loop and 5'-end (Figure 8), it seems likely that the two larger transcripts, 10.5kb and 11kb, contain additional untranslated sequence at either 5'-end or 3'-end. The two larger transcripts are not likely to be due to cross reaction between the NCKX5 probe and other NCKX family members since the probe used corresponds to the cytoplasmic loop of the mouse NCKX5 protein, which has very low sequence similarity to other NCKX family members. Furthermore, the pattern of expression observed for the two larger NCKX5 bands does not match those of previously identified NCKX family members (Tsoi, Rhee et al. 1998; Kraev, Quednau et al. 2001; Li, Kraev et al. 2002).

Probes from two different regions of NCKX5, one from the cytoplasmic loop and the other from the 5'-end, were also tested on mouse eye, skin and B16 cell line total RNA. Essentially, the results obtained with these two different probes were consistent (Figure 8). Both the larger two (11kb and 10.5kb) and the smaller two (1.6kb and 2.0kb) transcripts showed similar relative abundance in these tissues. The expression level of the 1.8kb transcript is as follow: B16>Eye>Skin. Nevertheless, the 10.5kb transcript from eye is very faint in the blot which was probed with the 5'-end probe. As the relative

intensity of 1.8kb transcript is also lower in the same blot compared to the blot using the cytoplasmic loop probe, it is likely the difference is due to different exposure time.

4.2 NCKX5 protein expression study

I was able to detect NCKX5 protein expression in transfected HEK293 cells, and the melanoma cell lines, B16 and MNT1, using a specific anti-NCKX5 serum. Two major bands were visible with sizes of 52kDa and 42kDa from all three preparations (Figure 9, 10, and 11). This is the first time the actual size of the NCKX5 protein has been reported. The results from N-glycosidase F digestion experiments suggest these two bands correspond to the same protein with different levels of glycosylation (Figure 12 and 13). From the immunoblot results on B16 and MNT1 cell preparations (Figure 10 and 11), it seems MNT1 cells mainly express NCKX5 protein of 52kDa whereas B16 cells mainly express NCKX5 protein of 42kDa. This difference may reflect different levels of modification, such as sialylation, at the same N-glycosylation site. The observation that these two cell lines express NCKX5 protein with different levels of glycosylation indicates these two forms of NCKX5 are at different processing stages, like Pmel 17, which is further processed by Golgi-resident enzymes after its original modification in the ER (Dell'Angelica 2003). As MNT1 cells are highly pigmented cells (Chi, Valencia et al. 2006) whereas B16 cells are not, it seems likely that the NCKX5 protein expressed in MNT1 cells represents the fully processed state of NCKX5.

In my study, I also tagged the NCKX5 protein at several sites with both FLAG and HA epitopes. The results of immunoblotting clearly demonstrated that I could detect all forms of NCKX5 protein expression in HEK293 cells with anti-NCKX5 serum (Figure 9).

However, I failed to detect any tagged NCKX5 protein expression in HEK293 cells using either anti-FLAG or anti-HA antibody. The reason that I could not detect N-terminal tagged protein might be that the tag was buried after protein glycosylation. But the reason why I could not detect NCKX5 tagged in the loop or at the C-terminus is not known. The size difference on SDS-PAGE (Figure 12) indicates the inserted epitope was present in the protein.

My immunoblot result showed the size of the NCKX5 protein without glycosylation was about 37kDa, which is significantly smaller than the predicted size of 52kDa. The most likely explanation for this observation is that the NCKX5 protein is highly hydrophobic. Therefore, it binds more SDS and runs faster than predicted for a protein of its size.

4.3 Subcellular localization study

This study revealed a similar subcellular localization pattern for recombinant NCKX5 protein expressed in transfected HEK293 cells and the endogenous NCKX5 protein expressed in B16 cells (Figure 14, 15, and 16). Both showed punctate staining mostly localized to the perinuclear region, but also present in lower levels throughout the cytoplasm. This staining pattern is different from the classic ER, Golgi, or mitochondria staining. Under higher magnification, it can be clearly seen that the staining corresponds to many tiny dots which may indicate that the stained proteins are enclosed in specialized vesicles or granules. This staining pattern is also somewhat different from the previously reported results in MNT1 cells, which showed NCKX5 staining throughout the entire cell body and less localized to the periphery of the nucleus (Lamason, Mohideen et al. 2005;

Chi, Valencia et al. 2006). This difference may simply be due to different cell types used in the experiments or different exposure of pictures. However, we have to bear in mind that in Cheng group's study (Lamason, Mohideen et al. 2005), the staining was done on MNT1 cells transfected with either GFP tagged or HA tagged NCKX5. In the overexpression system, the staining may not reflect the actual localization of native NCKX5 protein. Although I have also done some immunostaining experiments on MNT1 cells, the results are inconclusive, as our antibody only detected NCKX5 weakly.

4.4 NCKX5 function study

Although Cheng's group demonstrated NCKX5 could partially rescue the *golden* phenotype, no articles directly showing potassium-dependent sodium/calcium exchange activity from NCKX5, either *in vitro* or *in vivo*, have been published so far. Unfortunately, I was also unable to detect any sodium/calcium exchange activity from NCKX5 transfected HEK293 cell microsomes using the traditional Ca^{2+} uptake condition for NCX1 vesicles (Figure 17). Several other conditions, such as low pH inside vesicles, altered concentrations of monovalent cations, and lowered sucrose concentration inside vesicles, were also tried but generated similar results in which NCKX5 uptake activity could not be distinguished from the background level observed in vector transfected cells (data not shown). However, I did see Ca^{2+} uptake activity, which was time-, Na^+ concentration gradient-, and K^+-dependent in B16 and MNT1 cell microsome preparations under the same condition used for NCX1 uptake (Figure 18). Due to the lack of negative controls, I cannot confidently conclude the K^+-dependent Na^+/Ca^{2+} exchange activity I observed was due to NCKX5 expression, since I cannot totally exclude the

possibility that the observed activity is from other members of the NCKX family. The RT-PCR and immunoblot results (Figure 19) demonstrated that, besides NCKX5 expression, there were also NCKX4 and possible NCKX3 mRNA expression in B16 and MNT1 cells. However, my Ca^{2+} imaging data suggest there was no surface NCKX protein expression in those two cell lines. If the sodium/calcium exchange activity observed from B16 and MNT1 microsomes was due to NCKX5, then there are several possible reasons why no such activity was detected in NCKX5 transfected HEK293 cell microsomes. First, NCKX5 expressed in HEK293 cells may not be correctly folded. NCKX5 may require the binding of some ancillary protein(s), which only exist(s) in melanocytes, to be correctly folded and sorted. Second, NCKX5 may need to couple with other partner protein(s), which are localized on the membrane of melanosome together, to be fully functional.

As Cheng and colleague reported that the Ala111Thr polymorphism is associated with the lighter skin color in Caucasian people (Lamason, Mohideen et al. 2005), it is worthwhile testing the function of the protein carrying Ala111Thr. Since we don't have a reliable way to test the function of recombinant NCKX5 protein and the Ala111 residue is conserved among all known NCKX members, we mutated the corresponding alanine residue to threonine in NCKX4 (Ala125Thr), which is closer to NCKX5 than other members in NCKX family, and tested its function using Ca^{2+} imaging. This experiment was performed by Dr. Frank Visser. The results showed when the perfusion solution was switched from Na^{+}-containing to K^{+}- and Li^{+}-containing, the NCKX4 Ala125Thr mutant had only about half of Fura-2 ratio increase compared to the wild type one (data not shown), which indicates that the Ala125Thr change in NCKX4 reduced function

compared to wild type. This suggests the Ala111Thr polymorphism of NCKX5 may also have reduced function. However, further experiments conducted on NCKX5 are required to confirm this prediction.

A working model of NCKX5 was also proposed by the Cheng group (Lamason, Mohideen et al. 2005). Essentially, NCKX5 is coupled with V-type ATPase, which actively transports H^+ into melanosome to maintain the low pH environment inside melanosomes by hydrolyzing ATP, and Na^+/H^+ exchanger, which uses the H^+ concentration gradient across the membrane of melanosomes to accumulate Na^+ in melanosomes. NCKX5 utilizes this Na^+ concentration gradient to take Ca^{2+} into melanosomes. To test the hypothesized working model for NCKX5, Ca^{2+} imaging was also used. B16 or MNT1 cells were perfused with solution containing 1nM baflomycin, which is a specific V-type ATPase inhibitor, for the purpose of removing the energy source of this proposed transport network. If the proposed model is correct, we predicted Ca^{2+} release from melanosomes and consequently an increase in cytosolic Ca^{2+} concentration, and thus an increase in Fura-2 ratio. However, no such change was observed in our experiments (data not shown). This may indicate NCKX5 does not work as the model proposed. However, there are other possibilities for the failure to detect a Fura-2 ratio change. From the above result, we cannot conclude that NCKX5 is not coupled with V-type ATPase, and there are several possibilities for this observation. First, as the time to perfuse cells with baflomycin containing solution was only 2 minutes, it may not be long enough for baflomycin to reach the V-type ATPase and block its function. Second, we have no idea how long it takes for Ca^{2+} release from melanosomes after the function of V-type ATPase is inhibited. It is possible that the recording interval

is not suitable to monitor the Ca^{2+} release under this condition. Third, it is also possible that the rate of Ca^{2+} release from melanosomes is slower than the rate of Ca^{2+} sequestration or extrusion, hence no Fura-2 change could be observed. Last, most of the Ca^{2+} in melanosomes may be buffered and not readily releasable. Thus the amount of released Ca^{2+} was not enough to be reliably detected by Fura-2.

CHAPTER FIVE

FUTURE DIRECTIONS

The results obtained from this project revealed several basic properties of NCKX5, but there are lots of unknown aspects waiting to be discovered and understood. Several questions can be raised immediately from the results we obtained from this project. First, why does NCKX5 have two different sizes of transcripts to encode the same protein in different tissues? Second, what is the importance and implication of the two forms of glylcosylated NCKX5 protein? Is sorting or function of the NCKX5 protein affected by different levels of glycosylation? Third, is the Ca^{2+} uptake activity observed in B16 and MNT1 cell lines totally due to NCKX5? To test this idea, siRNA could be used to knock down the NCKX5 expression in these two cell lines. Membrane preparations from normal cells and NCKX5 knock down cells can be used in the Ca^{2+} uptake assay. It is also important to develop a reliable assay method to study the function of NCKX5 protein *in vitro*. Further questions could be addressed to the relationship of NCKX5 function and melanosome biogenesis. What processing and modification steps are involved in NCKX5 protein maturation? Which pathway is responsible for correctly sorting and transporting NCKX5 to melanosomes? The results of double staining experiments may give us some clues to this question. As we could detect NCKX activity from MNT1 and B16 microsomes but not from NCKX5 transfected HEK293 cell microsomes, it is natural to ask if there are other proteins involved in, or required for, NCKX5 function. Immunoprecipitation experiments could be conducted on B16 and MNT1 cells to investigate the partner protein(s) for NCKX5. And most important, what

physiological role does NCKX5 play in melanosome biogenesis? In order to answer these questions, a good understanding of both exchanger and melanosome maturation is required and beyond the scope of this project.

As a reduced function in NCKX4 with corresponding mutation Ala125Thr was recently observed in our lab, it is predicted that NCKX5 with Ala111Thr mutation has reduced activity too. Since the Ala111Thr polymorphism in human NCKX5 is also associated with the lighter skin color (Lamason, Mohideen et al. 2005), it is reasonable to postulate that other mutations with reduced function in NCKX5 may be related to some pathological states, such as albinism. Genetic analysis and sequencing of the NCKX5 gene of patients with albinism may discover the linkage of NCKX5 function and skin pigmentation. Mutagenesis and structure-function studies could also be introduced to identify the crucial residues for ion binding and transport of NCKX5 that may affect NCKX5 function. Ultimately, NCKX5 knock out mice and NCKX5 mutation knock in mice could be generated and the function of NCKX5 protein and the role it plays in melanosome biogenesis can be studied *in vivo*. The answers to all the questions will provide us a more complete understanding of melanosome biogenesis.

REFERENCES

Altimimi, H. F. and P. P. Schnetkamp (2007). "Na+-dependent inactivation of the retinal cone/brain Na+/Ca2+-K+ exchanger NCKX2." J Biol Chem **282**(6): 3720-9.

Ausubel, F. M. (2001). Current protocols in molecular biology. New York, J. Wiley.

Baker, P. F., M. P. Blaustein, et al. (1969). "The influence of calcium on sodium efflux in squid axons." J Physiol **200**(2): 431-58.

Berridge, M. J. (1998). "Neuronal calcium signaling." Neuron **21**(1): 13-26.

Berridge, M. J., M. D. Bootman, et al. (1998). "Calcium--a life and death signal." Nature **395**(6703): 645-8.

Berridge, M. J., M. D. Bootman, et al. (2003). "Calcium signalling: dynamics, homeostasis and remodelling." Nat Rev Mol Cell Biol **4**(7): 517-29.

Berridge, M. J., P. Lipp, et al. (2000). "The versatility and universality of calcium signalling." Nat Rev Mol Cell Biol **1**(1): 11-21.

Blaustein, M. P. and W. J. Lederer (1999). "Sodium/calcium exchange: its physiological implications." Physiol Rev **79**(3): 763-854.

Bootman, M. D. and M. J. Berridge (1995). "The elemental principles of calcium signaling." Cell **83**(5): 675-8.

Bootman, M. D., T. J. Collins, et al. (2001). "Calcium signalling--an overview." Semin Cell Dev Biol **12**(1): 3-10.

Cai, X., K. Zhang, et al. (2002). "A novel topology and redox regulation of the rat brain K+-dependent Na+/Ca2+ exchanger, NCKX2." J Biol Chem **277**(50): 48923-30.

Cai, X., K. Zhang, et al. (2002). "Topological studies of the rat brain K+-dependent Na+/Ca2+ exchanger NCKX2." Ann N Y Acad Sci **976**: 90-3.

Carstam, R., C. Brinck, et al. (1991). "The neuromelanin of the human substantia nigra." Biochim Biophys Acta **1097**(2): 152-60.

Cervetto, L., L. Lagnado, et al. (1989). "Extrusion of calcium from rod outer segments is driven by both sodium and potassium gradients." Nature **337**(6209): 740-3.

Chi, A., J. C. Valencia, et al. (2006). "Proteomic and bioinformatic characterization of the biogenesis and function of melanosomes." J Proteome Res **5**(11): 3135-44.

Cook, N. J. and U. B. Kaupp (1988). "Solubilization, purification, and reconstitution of the sodium-calcium exchanger from bovine retinal rod outer segments." J Biol Chem **263**(23): 11382-8.

Decressac, S., A. Grechez-Cassiau, et al. (2002). "Cloning, localization and functional properties of a cGMP-gated channel in photoreceptor cells from fish pineal gland." J Pineal Res **33**(4): 225-33.

Dell'Angelica, E. C. (2003). "Melanosome biogenesis: shedding light on the origin of an obscure organelle." Trends Cell Biol **13**(10): 503-6.

Dell'Angelica, E. C., C. Mullins, et al. (2000). "Lysosome-related organelles." Faseb J **14**(10): 1265-78.

Dong, H., P. E. Light, et al. (2001). "Electrophysiological characterization and ionic stoichiometry of the rat brain K(+)-dependent NA(+)/CA(2+) exchanger, NCKX2." J Biol Chem **276**(28): 25919-28.

Drager, U. C. (1985). "Calcium binding in pigmented and albino eyes." Proc Natl Acad Sci U S A **82**(19): 6716-20.

Feske, S., Y. Gwack, et al. (2006). "A mutation in Orai1 causes immune deficiency by abrogating CRAC channel function." Nature **441**(7090): 179-85.

Gyorke, I., N. Hester, et al. (2004). "The role of calsequestrin, triadin, and junctin in conferring cardiac ryanodine receptor responsiveness to luminal calcium." Biophys J **86**(4): 2121-8.

Hearing, V. J. (2005). "Biogenesis of pigment granules: a sensitive way to regulate melanocyte function." J Dermatol Sci **37**(1): 3-14.

Hess, H. H. (1975). "The high calcium content of retinal pigmented epithelium." Exp Eye Res **21**(5): 471-9.

Honing, S., I. V. Sandoval, et al. (1998). "A di-leucine-based motif in the cytoplasmic tail of LIMP-II and tyrosinase mediates selective binding of AP-3." Embo J **17**(5): 1304-14.

Izagirre, N., I. Garcia, et al. (2006). "A scan for signatures of positive selection in candidate loci for skin pigmentation in humans." Mol Biol Evol **23**(9): 1697-706.

Jackson, I. J. (2006). "Identifying the genes causing human diversity." Eur J Hum Genet **14**(9): 979-80.

Jimbow, K., J. S. Park, et al. (2000). "Assembly, target-signaling and intracellular transport of tyrosinase gene family proteins in the initial stage of melanosome biogenesis." Pigment Cell Res **13**(4): 222-9.

Kang, K. J., T. G. Kinjo, et al. (2005). "Residues contributing to the Ca2+ and K+ binding pocket of the NCKX2 Na+/Ca2+-K+ exchanger." J Biol Chem **280**(8): 6823-33.

Kang, K. J., Y. Shibukawa, et al. (2005). "Substitution of a single residue, Asp575, renders the NCKX2 K+-dependent Na+/Ca2+ exchanger independent of K+." J Biol Chem **280**(8): 6834-9.

Kinjo, T. G., K. Kang, et al. (2005). "Site-directed disulfide mapping of residues contributing to the Ca2+ and K+ binding pocket of the NCKX2 Na+/Ca2+-K+ exchanger." Biochemistry **44**(21): 7787-95.

Kinjo, T. G., R. T. Szerencsei, et al. (2003). "Topology of the retinal cone NCKX2 Na/Ca-K exchanger." Biochemistry **42**(8): 2485-91.

Kobayashi, T., K. Urabe, et al. (1994). "The Pmel 17/silver locus protein. Characterization and investigation of its melanogenic function." J Biol Chem **269**(46): 29198-205.

Kong, H., R. Wang, et al. (2007). "Skeletal and Cardiac Ryanodine Receptors Exhibit Different Responses to Ca2+ Overload and Luminal Ca2+." Biophys J.

Kongshoj, B., A. Thorleifsson, et al. (2006). "Pheomelanin and eumelanin in human skin determined by high-performance liquid chromatography and its relation to in vivo reflectance measurements." Photodermatol Photoimmunol Photomed **22**(3): 141-7.

Kraev, A., B. D. Quednau, et al. (2001). "Molecular cloning of a third member of the potassium-dependent sodium-calcium exchanger gene family, NCKX3." J Biol Chem **276**(25): 23161-72.

Kushimoto, T., V. Basrur, et al. (2001). "A model for melanosome biogenesis based on the purification and analysis of early melanosomes." Proc Natl Acad Sci U S A **98**(19): 10698-703.

Lamason, R. L., M. A. Mohideen, et al. (2005). "SLC24A5, a putative cation exchanger, affects pigmentation in zebrafish and humans." Science **310**(5755): 1782-6.

Laver, D. R. (2006). "Regulation of ryanodine receptors from skeletal and cardiac muscle during rest and excitation." Clin Exp Pharmacol Physiol **33**(11): 1107-13.

Lee, J. Y., F. Visser, et al. (2006). "Protein kinase C-dependent enhancement of activity of rat brain NCKX2 heterologously expressed in HEK293 cells." J Biol Chem **281**(51): 39205-16.

Lennarz, W. J. and M. D. Lane (2004). Encyclopedia of biological chemistry. Amsterdam; Boston, Elsevier.

Li, X. F., L. Kiedrowski, et al. (2006). "Importance of K+-dependent Na+/Ca2+-exchanger 2, NCKX2, in motor learning and memory." J Biol Chem **281**(10): 6273-82.

Li, X. F., A. S. Kraev, et al. (2002). "Molecular cloning of a fourth member of the potassium-dependent sodium-calcium exchanger gene family, NCKX4." J Biol Chem **277**(50): 48410-7.

Li, Z., S. Matsuoka, et al. (1994). "Cloning of the NCX2 isoform of the plasma membrane Na(+)-Ca2+ exchanger." J Biol Chem **269**(26): 17434-9.

Liou, J., M. L. Kim, et al. (2005). "STIM is a Ca2+ sensor essential for Ca2+-store-depletion-triggered Ca2+ influx." Curr Biol **15**(13): 1235-41.

Lytton, J. (2002). "How many sodium ions does it take to turn an exchanger?" J Physiol **545**(Pt 2): 335.

Lytton, J., X. F. Li, et al. (2002). "K+-dependent Na+/Ca2+ exchangers in the brain." Ann N Y Acad Sci **976**: 382-93.

Marks, M. S. and M. C. Seabra (2001). "The melanosome: membrane dynamics in black and white." Nat Rev Mol Cell Biol **2**(10): 738-48.

Maruyama, K. and D. H. MacLennan (1988). "Mutation of aspartic acid-351, lysine-352, and lysine-515 alters the Ca2+ transport activity of the Ca2+-ATPase expressed in COS-1 cells." Proc Natl Acad Sci U S A **85**(10): 3314-8.

Nicoll, D. A., S. Longoni, et al. (1990). "Molecular cloning and functional expression of the cardiac sarcolemmal Na(+)-Ca2+ exchanger." Science **250**(4980): 562-5.

Nicoll, D. A., B. D. Quednau, et al. (1996). "Cloning of a third mammalian Na+-Ca2+ exchanger, NCX3." J Biol Chem **271**(40): 24914-21.

Norton, H. L., R. A. Kittles, et al. (2006). "Genetic Evidence for the Convergent Evolution of Light Skin in Europeans and East Asians." Mol Biol Evol.

Okazaki, Y., M. Furuno, et al. (2002). "Analysis of the mouse transcriptome based on functional annotation of 60,770 full-length cDNAs." Nature **420**(6915): 563-73.

Panessa, B. J. and J. A. Zadunaisky (1981). "Pigment granules: a calcium reservoir in the vertebrate eye." Exp Eye Res **32**(5): 593-604.

Petersen, O. H. (2002). "Calcium signal compartmentalization." Biol Res **35**(2): 177-82.

Philipson, K. D. and D. A. Nicoll (2000). "Sodium-calcium exchange: a molecular perspective." Annu Rev Physiol **62**: 111-33.

Porzig, H., Z. Li, et al. (1993). "Mapping of the cardiac sodium-calcium exchanger with monoclonal antibodies." Am J Physiol **265**(3 Pt 1): C748-56.

Quednau, B. D., D. A. Nicoll, et al. (1997). "Tissue specificity and alternative splicing of the Na+/Ca2+ exchanger isoforms NCX1, NCX2, and NCX3 in rat." Am J Physiol **272**(4 Pt 1): C1250-61.

Reeves, J. P. and J. L. Sutko (1979). "Sodium-calcium ion exchange in cardiac membrane vesicles." Proc Natl Acad Sci U S A **76**(2): 590-4.

Reeves, J. P. and J. L. Sutko (1983). "Competitive interactions of sodium and calcium with the sodium-calcium exchange system of cardiac sarcolemmal vesicles." J Biol Chem **258**(5): 3178-82.

Reilander, H., A. Achilles, et al. (1992). "Primary structure and functional expression of the Na/Ca,K-exchanger from bovine rod photoreceptors." Embo J **11**(5): 1689-95.

Reuter, H. and N. Seitz (1968). "The dependence of calcium efflux from cardiac muscle on temperature and external ion composition." J Physiol **195**(2): 451-70.

Roos, J., P. J. DiGregorio, et al. (2005). "STIM1, an essential and conserved component of store-operated Ca2+ channel function." J Cell Biol **169**(3): 435-45.

Rossi, A. E. and R. T. Dirksen (2006). "Sarcoplasmic reticulum: the dynamic calcium governor of muscle." Muscle Nerve **33**(6): 715-31.

Salceda, R. and J. R. Riesgo-Escovar (1990). "Characterization of calcium uptake in chick retinal pigment epithelium." Pigment Cell Res **3**(3): 141-5.

Salceda, R. and G. Sanchez-Chavez (2000). "Calcium uptake, release and ryanodine binding in melanosomes from retinal pigment epithelium." Cell Calcium **27**(4): 223-9.

Sambrook, J. (2001). Molecular cloning: a laboratory manual. Cold Spring Harbor, N.Y., Cold Spring Harbor Laboratory Press.

Schnetkamp, P. P. (2004). "The SLC24 Na+/Ca2+-K+ exchanger family: vision and beyond." Pflugers Arch **447**(5): 683-8.

Sharma, S., S. Wagh, et al. (2002). "Melanosomal proteins--role in melanin polymerization." Pigment Cell Res **15**(2): 127-33.

Soboloff, J., M. A. Spassova, et al. (2006). "Calcium signals mediated by STIM and Orai proteins--a new paradigm in inter-organelle communication." Biochim Biophys Acta **1763**(11): 1161-8.

Soejima, M. and Y. Koda (2007). "Population differences of two coding SNPs in pigmentation-related genes SLC24A5 and SLC45A2." Int J Legal Med **121**(1): 36-9.

Strehler, E. E. and M. Treiman (2004). "Calcium pumps of plasma membrane and cell interior." Curr Mol Med **4**(3): 323-35.

Szerencsei, R. T., R. J. Winkfein, et al. (2002). "The Na/Ca-K exchanger gene family." Ann N Y Acad Sci **976**: 41-52.

Tsoi, M., K. H. Rhee, et al. (1998). "Molecular cloning of a novel potassium-dependent sodium-calcium exchanger from rat brain." J Biol Chem **273**(7): 4155-62.

Visser, F., V. Valsecchi, et al. (2006). "Analysis of Ion Interactions with the K+-dependent Na+/Ca2+ exchangers NCKX2, NCKX3 and NCKX4: Identification of T551 as a key residue in defining the apparent K+ affinity of NCKX2." J Biol Chem.

Yoo, S. S., S. Leach, et al. (2002). "Studies on the oligomeric state of the sodium/calcium + potassium exchanger NCKX2." Ann N Y Acad Sci **976**: 94-6.